Quasiparticle and phonon lifetimes in superconductors*

S. B. Kaplan, C. C. Chi, and D. N. Langenberg
Department of Physics and Laboratory for Research on the Structure of Matter, University of Pennsylvania, Philadelphia, Pennsylvania 19174

J. J. Chang, S. Jafarey, and D. J. Scalapino
Department of Physics, University of California, Santa Barbara, California 93106

(Received 1 June 1976)

Low-energy quasiparticle scattering, recombination, and branch-mixing lifetimes and phonon pair-breaking and scattering lifetimes are calculated for superconductors. The quasiparticle calculations relate these lifetimes to the low-frequency behavior of $\alpha^2(\Omega)F(\Omega)$. Results are obtained using the low-frequency approximate form $\alpha^2(\Omega)F(\Omega) = b\Omega^2$, with b determined from electron tunneling measurements. For the strong-coupling superconductors Pb and Hg, the full tunneling form for $\alpha^2(\Omega)F(\Omega)$ is used. The phonon lifetimes are shown to depend on $\alpha^2(\Omega)$. Results are compared with experiment.

I. INTRODUCTION

The lifetimes of low-energy quasiparticles and phonons enter into a variety of phenomena in superconductors nearly in thermal equilibrium. Furthermore, an understanding and an accurate parametrization of the interactions responsible for these lifetimes are essential for the development of a theory of the nonequilibrium superconductor, e.g., a superconducting film strongly perturbed by photons, phonons, or a large injected quasiparticle current.[1] We describe here the results of a study of the near-equilibrium lifetimes of elementary excitations in superconductors, motivated by our interest in the nonequilibrium problem.

In most superconductors, the dominant quasiparticle relaxation processes are inelastic scattering with phonons and recombination with phonon emission to form bound Cooper pairs. Direct electron-electron scattering processes eventually dominate at sufficiently low energies and can be significant for metals with large Debye energies and low superconducting transition temperatures, such as Al. In this paper we will focus on the contributions of inelastic phonon processes to quasiparticle relaxation lifetimes. Various derivations for these lifetimes as well as certain analytic results and some numerical calculations exist in the literature.[2-6] Here we seek to provide a unified and self-contained discussion which gives accurate lifetime estimates for comparison with experimental results for real metals.

In most metals, the lifetimes of low-energy quasiparticles can be related to the low-frequency part of the phonon density of states $F(\Omega)$ weighted by the square of the matrix element of the electron-phonon interaction $\alpha^2(\Omega)$. In Sec. II we review the calculation of the lifetime of a quasiparticle in terms of $\alpha^2(\Omega)F(\Omega)$ for a superconductor in thermodynamic equilibrium. We separate the decay rate into scattering and recombination rates which define the scattering and recombination lifetimes, respectively. We conclude this section by discussing the strength of the electron-electron scattering. Such processes enter into determining the low-energy quasiparticle lifetimes in materials with large Debye energies.[7,8]

In Sec. III we present results for the lifetimes based on currently available information on $\alpha^2(\Omega)F(\Omega)$. For a simple model of a metal, $\alpha^2(\Omega)F(\Omega)$ can be approximated at low frequencies by the quadratic form $b\Omega^2$. In principle, superconducting tunneling measurements[9] provide direct information on $\alpha^2(\Omega)F(\Omega)$. However, the tunneling data are insensitive to the form of the interaction at very low frequencies and the $\alpha^2(\Omega)F(\Omega)$ experimentally determined at large Ω is usually fitted to $b\Omega^2$ at small Ω.[10] We calculate scattering and recombination lifetimes using this approximate form, which should be applicable to many superconductors. In addition, we present results for the strong-coupling superconductors Pb and Hg obtained by using the full experimentally determined $\alpha^2(\Omega)F(\Omega)$, which shows significant low-frequency structure. To our knowledge this is the first published calculation of lifetimes using the tunneling $\alpha^2(\Omega)F(\Omega)$ data.[11]

When the $k < k_F$ and $k > k_F$ (k_F is the Fermi wave vector) branches of the quasiparticle excitation curve are unequally populated, another characteristic quasiparticle lifetime enters, the branch-mixing time.[12-15] The inelastic scattering events which contribute to this time are those quasiparticle scattering and recombination events which relax a branch imbalance. In Sec. IV we present results for the branch-mixing time.

For the phonons in a superconductor with ener-

gies much less than the Debye energy, lifetimes may be calculated for quasiparticle scattering and for breaking of Cooper pairs. In Sec. V we show how these lifetimes are related to $\alpha^2(\Omega)$ and present some quantitative results for them. In Sec. VI we compare our various theoretical results with experiment.

We emphasize at the outset that our calculations are for quasiparticles and phonons in a dirty superconductor in or very near thermal equilibrium and yield energy-dependent lifetimes. The effective lifetimes measured experimentally in a nonequilibrium superconductor generally represent some average over quasiparticle and phonon energy distributions which may deviate strongly from the corresponding equilibrium distributions. This should be borne in mind in attempting to apply our results to experimental situations.

II. FORMULATION

The poles of the single-particle Green's function in the superconducting state are determined by

$$Z^2(\omega)\omega^2 - \epsilon_p^2 - \phi^2(\omega) = 0\,, \tag{1}$$

where $Z(\omega)$ is the renormalization parameter, and $\phi(\omega)$ is the gap parameter. According to the Eliashberg formulation[16,17]

$$[1-Z(\omega)]\omega = \int_0^\infty d\omega'\,\mathrm{Re}\left(\frac{\omega'}{[\omega'^2-\Delta^2(\omega')]^{1/2}}\right) \times \int_0^\infty d\Omega\,\alpha^2(\Omega)F(\Omega)\left(\frac{f(-\omega')+n(\Omega)}{\omega'+\omega+\Omega+i\delta} - \frac{f(-\omega')+n(\Omega)}{\omega'-\omega+\Omega-i\delta} + \frac{f(\omega')+n(\Omega)}{-\omega'+\omega+\Omega+i\delta} - \frac{f(\omega')+n(\Omega)}{-\omega'-\omega+\Omega-i\delta}\right), \tag{2a}$$

$$\phi(\omega) = \int_0^\infty d\omega'\,\mathrm{Re}\left(\frac{\Delta(\omega')}{[\omega'^2-\Delta^2(\omega')]^{1/2}}\right) \int_0^\infty d\Omega\,\alpha^2(\Omega)F(\Omega) \times\left(\frac{f(-\omega')+n(\Omega)}{\omega'+\omega+\Omega+i\delta} + \frac{f(-\omega')+n(\Omega)}{\omega'-\omega+\Omega-i\delta} - \frac{f(\omega')+n(\Omega)}{-\omega'+\omega+\Omega+i\delta} - \frac{f(\omega')+n(\Omega)}{-\omega'-\omega+\Omega-i\delta}\right)$$
$$-\mu^* \int_0^{\omega_c} d\omega'\,\mathrm{Re}\left(\frac{\Delta(\omega')}{[\omega'^2-\Delta^2(\omega')]^{1/2}}\right)\tanh\left(\frac{\beta\omega'}{2}\right). \tag{2b}$$

Here μ^* is the Coulomb pseudopotential, ω_c is a cutoff frequency of order ω_D, and $\Delta(\omega)=\phi(\omega)/Z(\omega)$. The spectral weight $\alpha^2(\Omega)F(\Omega)$ is given by averaging the square of the dressed electron-phonon matrix element for a fixed phonon energy Ω and all polarizations λ over the Fermi surface,

$$\alpha^2(\Omega)F(\Omega) = \left(\sum_\lambda \int dp^2 \int \frac{dp'^2}{(2\pi)^3 v_F} |\bar{g}_{p-p',\lambda}|^2 \delta(\Omega-\omega_{p-p',\lambda})\right)\left(\int dp^2\right)^{-1}. \tag{3}$$

Setting $\omega = E(\omega) - i\Gamma(\omega)$, $Z(\omega)=Z_1(\omega)+iZ_2(\omega)$, and $\phi(\omega)=\phi_1(\omega)+i\phi_2(\omega)$, and assuming that the imaginary parts are small compared to the real parts, one finds from Eq. (1) that

$$\Gamma(\omega) = \omega Z_2(\omega)/Z_1(\omega) - \phi_1(\omega)\phi_2(\omega)/Z_1^2(\omega)\omega\,. \tag{4}$$

The real and imaginary parts of Z and ϕ are to be obtained from Eqs. (2a) and (2b).[18] The inverse of the lifetime, the decay rate $\tau^{-1}(\omega)$ of a quasiparticle of energy ω, is equal to $2\Gamma(\omega)$. For frequencies small compared with typical phonon frequencies, we neglect the frequency dependence of Z_1 and ϕ_1, setting $Z_1(\omega)\cong Z_1(\Delta_0)\cong Z_1(0)$ and $\phi_1(\omega)/Z_1(\omega)\cong\phi_1(\Delta_0)/Z_1(\Delta_0)\equiv\Delta_0$. Here Δ_0 is the usual temperature-dependent energy gap, which we will henceforth simply denote by Δ. We also neglect the temperature dependence of $Z_1(0)$. With these approximations, Eq. (4) reduces to

$$\Gamma(\omega) = \omega Z_2(\omega)/Z_1 - (\Delta/\omega)\phi_2(\omega)/Z_1\,. \tag{5}$$

In the same spirit, we replace $\Delta(\omega)$ by Δ in determining $Z_2(\omega)$ and $\phi_2(\omega)$ from Eqs. (2a) and (2b). The inverse lifetime $\tau(\omega)$ of a quasiparticle of energy ω can then be written[19]

$$\tau^{-1}(\omega) = 2\Gamma(\omega) = \frac{2\pi}{\hbar Z_1(0)}\int_0^{\omega-\Delta} d\Omega\,\alpha^2(\Omega)F(\Omega)\,\mathrm{Re}\left(\frac{\omega-\Omega}{[(\omega-\Omega)^2-\Delta^2]^{1/2}}\right)\left(1-\frac{\Delta^2}{\omega(\omega-\Omega)}\right)[f(\Omega-\omega)+n(\Omega)]$$
$$+\frac{2\pi}{\hbar Z_1(0)}\int_{\omega+\Delta}^\infty d\Omega\,\alpha^2(\Omega)F(\Omega)\,\mathrm{Re}\left(\frac{\Omega-\omega}{[(\Omega-\omega)^2-\Delta^2]^{1/2}}\right)\left(1+\frac{\Delta^2}{\omega(\Omega-\omega)}\right)[f(-\omega+\Omega)+n(\Omega)]$$
$$+\frac{2\pi}{\hbar Z_1(0)}\int_0^\infty d\Omega\,\alpha^2(\Omega)F(\Omega)\,\mathrm{Re}\left(\frac{\omega+\Omega}{[(\omega+\Omega)^2-\Delta^2]^{1/2}}\right)\left(1-\frac{\Delta^2}{\omega(\Omega+\omega)}\right)[f(\omega+\Omega)+n(\Omega)]. \tag{6}$$

Using identities of the type

$$f(\Omega+\omega)+n(\Omega)=[1-f(\omega)]^{-1}n(\Omega)[1-f(\Omega+\omega)], \tag{7}$$

the inverse lifetime $\tau^{-1}(\omega)$, Eq. (6), can be expressed in the more familiar form

$$\tau^{-1}(\omega)=\frac{2\pi}{\hbar Z_1(0)[1-f(\omega)]}\left[\int_0^{\omega-\Delta} d\Omega\,\alpha^2(\Omega)F(\Omega)\,\mathrm{Re}\left(\frac{\omega-\Omega}{[(\omega-\Omega)^2-\Delta^2]^{1/2}}\right)\left(1-\frac{\Delta^2}{\omega(\omega-\Omega)}\right)[n(\Omega)+1][1-f(\omega-\Omega)]\right.$$
$$+\int_{\omega+\Delta}^{\infty} d\Omega\,\alpha^2(\Omega)F(\Omega)\,\mathrm{Re}\left(\frac{\Omega-\omega}{[(\Omega-\omega)^2-\Delta^2]^{1/2}}\right)\left(1+\frac{\Delta^2}{\omega(\Omega-\omega)}\right)[n(\Omega)+1]f(\Omega-\omega)$$
$$\left.+\int_0^{\infty} d\Omega\,\alpha^2(\Omega)F(\Omega)\,\mathrm{Re}\left(\frac{\omega+\Omega}{[(\omega+\Omega)^2-\Delta^2]^{1/2}}\right)\left(1-\frac{\Delta^2}{\omega(\Omega+\omega)}\right)n(\Omega)[1-f(\Omega+\omega)]\right]. \tag{8}$$

Examination of the Fermi and Bose factors as well as the energy variables and coherence factors in Eq. (8) shows that the first and the third terms correspond to quasiparticle scattering processes with the emission and absorption of a phonon, respectively. We will denote this part of the transition rate as $\tau_s^{-1}(\omega)$. The second term corresponds to a process in which the quasiparticle recombines with another quasiparticle to form a pair with the excess energy emitted as a phonon. This gives rise to the recombination rate τ_r^{-1}. The factor Z_1^{-1} in Eqs. (6) and (8) renormalizes the electron-phonon interaction and can be interpreted as follows: The interaction was computed using Bloch states, but the fraction of the initial quasiparticle state in this Bloch state is given by the wave-function renormalization factor $Z_1^{-1/2}$. The remaining parts of the state consist of a superposition of virtually scattered electrons and phonons. Since all parts of the spectrum of the final state are summed over, only $Z_1^{-1/2}$ enters in reducing the matrix element, and when this is squared one gets Z_1^{-1}. The factor $[1-f(\omega)]^{-1}$ represents an enhancement of the decay rate due to the Pauli-principle blocking of the backscattering of other quasiparticles into the occupied quasiparticle state of energy ω. Similar forms for these lifetimes can be obtained using the golden rule.

Clearly, for $\omega \sim kT_c$ and $T \leq T_c$, only the low-frequency ($\Omega \sim kT_c$) part of α^2F enters in determining $\tau(\omega)$. As is well known, at sufficiently low frequencies the effective electron-phonon coupling constant $\alpha^2(\Omega)$ approaches a constant, and $\alpha^2(\Omega)F(\Omega)$ is proportional to Ω^2, reflecting the rise of the phonon density of states.[9,17,20] However, as Ω increases, becoming larger than the phonon frequencies ω_{q^*} associated with wave vectors q^* of order of the separation between pieces of the Fermi surface at zone boundaries, umklapp processes become important. For systems with nearly spherical Fermi surfaces, the umklapp processes provide the mechanism for coupling to the transverse phonons, which can have a significantly larger density of states than the longitudinal phonons. In addition, the single-orthogonalized-plane-wave (OPW) approximation for umklapp gives $\alpha^2 \sim \Omega^{-1}$. Here we will proceed in two ways: (i) assume that $\alpha^2(\Omega)F(\Omega) \propto \Omega^2$, with the proportionality constant determined by a fit to the tunneling data; (ii) take the full experimental numerical form for $\alpha^2(\Omega)F(\Omega)$. This second procedure is of interest for systems such as Pb and Hg which have structure in $\alpha^2(\Omega)F(\Omega)$ at small Ω.

Direct electron-electron scattering processes can also contribute to quasiparticle lifetimes,[7,8] together with processes in which inelastic energy transfer is associated with emission or absorption of real phonons: In addition to the screened Coulomb interaction, the direct electron-electron interaction can be mediated by virtual phonons. As Gray[7] has emphasized, electron-electron scattering can play a significant role in metals with large Debye temperatures. In a normal metal, the final-state phase space for an electron of energy ω scattering to a final state consisting of two electrons and a hole varies as ω/μ, where μ is the Fermi energy. Thus, at sufficiently low energies the *total* effective $\alpha^2(\Omega)F(\Omega)$ should vary linearly rather than quadratically with Ω. To estimate the importance of the electron-electron scattering we note the well-known results for normal metals: At zero temperature, quasiparticle relaxation rates vary as ω^2/μ and ω^3/ω_D^2 for direct electron-electron and phonon-emission processes, respectively. These became equal for $\omega=\omega_D^2/\mu$. In Table I we list values of ω_D^2/μ for various metals. Except for Al and Zn, all of the values are small compared with excitation energies of order kT_c.

III. RESULTS FOR QUASIPARTICLE SCATTERING AND RECOMBINATION LIFETIMES

Here we present results for the scattering or thermalization quasiparticle lifetime $\tau_s(\omega, T)$ and the recombination lifetime $\tau_r(\omega, T)$. First we treat the situation in which $\alpha^2(\Omega)F(\Omega)$ is approximated by its low-frequency form

TABLE I. Characteristic quasiparticle times and associated parameters. All data are taken from Ref. 9 unless otherwise referenced.

Metal	T_c (K)	ω_D [a] (K)	μ [a] (K)	ω_D^2/μ (K)	$\hbar^2\omega_D^2/\mu k T_c$	$Z_1(0)$	$\alpha^2(2\Delta(0))F(2\Delta(0))$	$10^3 b$ (meV^{-2})	$10^9\tau_0$ (sec)
Pb	7.19	105	10.9	0.101	0.0141	2.55	0.154	5.72	0.196
In	3.40	108	10.0	0.117	0.0344	1.81	0.0110	9.43	0.799
Sn	3.75	200	11.6	0.344	0.0916	1.72	0.003 41	2.32	2.30
Hg	4.19	71.9	8.29	0.0624	0.0149	2.63	0.564	78.4	0.0747
Tl	2.33	78.5	9.46	0.0651	0.028	1.80	0.007 09	13.2	1.76
Ta	4.48	240	18.0	0.321	0.0715	1.69	0.003 60	1.73	1.78
Nb [b]	9.2	275	6.18	1.22	0.133	2.84	0.037	4.0	0.149
Al [c]	1.19	428	13.5	1.36	1.14	1.43	0.000 039 3	0.317	438.
Zn [d]	0.875	327	10.9	0.981	1.12	1.34	0.000 024 2	0.420	780.
$Pb_{60}Tl_{40}$	6.0					2.38	0.132	27.9	0.0647
$Pb_{40}Tl_{60}$	4.7					2.15	0.0744	28.7	0.118
$Pb_{60}Bi_{20}Tl_{20}$	7.26					2.81	0.661	21.2	0.0567
$Pb_{90}Bi_{10}$	7.55–8.05					2.66	0.564	21.4	0.043

[a] Data for ω_D and μ are from Ref. 21.

[b] Estimates were obtained by normalizing to 3 the neutron data for $F(\Omega)$ of Ref. 22 and assuming a constant α^2 and $\lambda = 1.84$ (Ref. 23).

[c] These data were taken from the four-OPW calculations of $\alpha^2(\Omega)F(\Omega)$ of Carbotte and Tomlinson (Ref. 24) which make use of a many-nearest-neighbor Born–von Kármán fit to neutron data in order to extract the Fermi-surface-averaged phonon density of states. In principle, the multi-OPW nature of the calculation should result in the proper behavior of the function at low energies. However, the authors referenced were not primarily interested in this range of energies, and their results show considerable scatter for energies less than approximately 1 meV. We have made a quadratic fit to their results to find b.

[d] These data are from the four-OPW calculations of Swihart and Tomlinson (Ref. 25). A quadratic fit was once again needed for the low-energy data. We strongly urge that in future calculations, particular attention be paid to the range of energies of interest in this paper, since b from our present fit is at best good to 20%.

$$\alpha^2(\Omega)F(\Omega) = b\Omega^2 . \tag{9}$$

Here b is a constant characteristic of a given material. Results for b obtained from superconducting tunneling experiments are listed in Table I, together with several values from theoretical calculations.

The results for the lifetimes can be plotted in a universal form with the lifetimes measured in units of time

$$\tau_0 = Z_1(0)\hbar/2\pi b(kT_c)^3 . \tag{10}$$

Values of this characteristic time τ_0 for different metals are listed in Table I. In Figs. 1 and 2 results for $\tau_s(\omega, T)/\tau_0$ and $\tau_r(\omega, T)/\tau_0$, respectively, are plotted versus T/T_c for various values of ω. In obtaining these universal curves we have used the weak-coupling relation $2\Delta(0)kT_c = 3.52$. For a quasiparticle at the gap edge $[\omega = \Delta(T)]$, the integrals in Eq. (8) can be expressed in terms of an infinite series involving the modified Bessel functions K_0 and K_1:

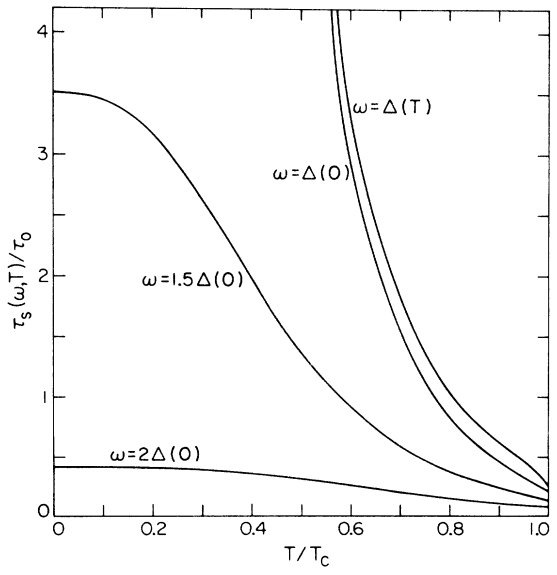

FIG. 1. Scattering lifetime τ_s in units of τ_0 vs T/T_c for quasiparticles with different excitation energies ω. Table I lists τ_0 for various metals. These curves were obtained using the approximation $\alpha^2(\Omega)F(\Omega) = b\Omega^2$.

$$\tau_r^{-1}(\Delta(T)) = \tau_0^{-1}\left(\frac{\Delta}{kT_c}\right)^3 \sum_{n=1}^{\infty}\left[(-1)^{n+1} + \exp\left(\frac{-n\Delta}{kT}\right)\right]\left\{\left[4 + \frac{3kT}{n\Delta} + 2\left(\frac{kT}{n\Delta}\right)^2\right]K_1\left(\frac{n\Delta}{kT}\right) + \left(4 + \frac{kT}{n\Delta}\right)K_0\left(\frac{n\Delta}{kT}\right)\right\}, \tag{11}$$

$$\tau_s^{-1}(\Delta(T)) = \tau_0^{-1}\left(\frac{\Delta}{kT_c}\right)^3 \sum_{n=1}^{\infty}\left[(-1)^{n+1} + \exp\left(\frac{n\Delta}{kT}\right)\right]\left\{\left[4 - \frac{3kT}{n\Delta} + 2\left(\frac{kT}{n\Delta}\right)^2\right]K_1\left(\frac{n\Delta}{kT}\right) - \left(4 - \frac{kT}{n\Delta}\right)K_0\left(\frac{n\Delta}{kT}\right)\right\}. \tag{12}$$

These series are rapidly convergent at low temperatures. The leading low-temperature behavior is

$$\tau_0/\tau_s^{-1}(\Delta, T) \cong \Gamma(\tfrac{7}{2})\zeta(\tfrac{7}{2})\left(\frac{kT_c}{2\Delta(0)}\right)^{1/2}\left(\frac{T}{T_c}\right)^{7/2}, \tag{13}$$

$$\tau_0/\tau_r^{-1}(\Delta, T) \cong (\pi)^{1/2}\left(\frac{2\Delta(0)}{kT_c}\right)^{5/2}\left(\frac{T}{T_c}\right)^{1/2} e^{-\Delta(0)/kT}. \tag{14}$$

If the $b\Omega^2$ form of $\alpha^2(\Omega)F(\Omega)$ is not valid for $\Omega \approx 2\Delta(0)$, one may use the more general low-temperature approximation for τ_r:

$$\tau_r^{-1}(\Delta, T) \cong [4\pi\Delta(0)\alpha^2(2\Delta(0))F(2\Delta(0))/\hbar Z_1(0)][\pi kT/2\Delta(0)]^{1/2} e^{-\Delta(0)/kT}. \tag{15}$$

Values for $\alpha^2(2\Delta(0))F(2\Delta(0))$ are listed in Table I. A corresponding expression for τ_s is unnecessary because for quasiparticle scattering processes the important phonon energies are near zero, not $2\Delta(0)$, so that the $b\Omega^2$ approximation result [Eq. (13)] remains valid even if $b\Omega^2$ is not a good approximation to $\alpha^2(\Omega)F(\Omega)$ for $\Omega \sim 2\Delta(0)$.

The scattering lifetime $\tau_s(\omega, T)$ increases as the temperature is lowered owing to a decrease in the thermal phonon population. A quasiparticle at the gap edge, $\omega = \Delta(T)$, cannot emit a phonon and scatter because it is in the lowest-energy quasiparticle state. For this reason $\tau_s(\Delta(T), T)$ increases when T decreases as shown in Fig. 1 and Eq. (13). However, for quasiparticles with energies $\omega > \Delta(T)$, spontaneous phonon emission sets a limit to the scattering lifetime τ_s. This effect is clearly seen in Fig. 1 for the cases $\omega = 1.5\Delta(0)$ and $2\Delta(0)$. This limiting value for the scattering lifetime is

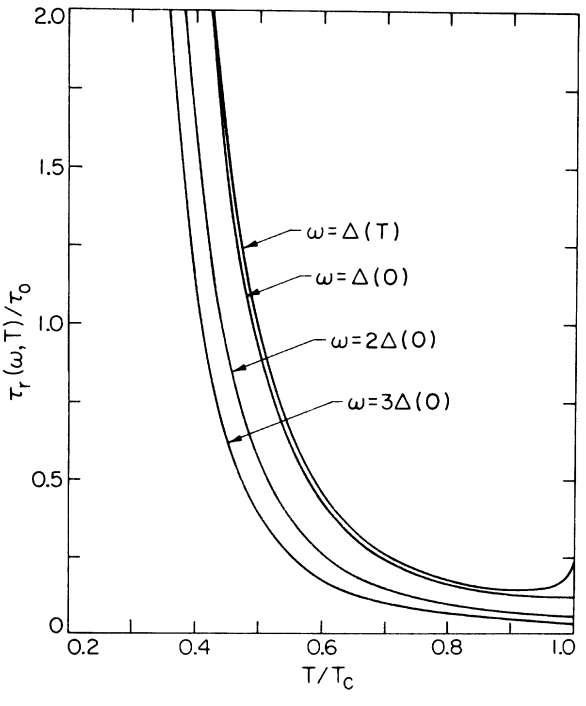

FIG. 2. Recombination lifetime τ_r in units of τ_0 (see Table I) vs T/T_c for quasiparticles with various excitation energies ω. These curves were obtained using the approximation $\alpha^2(\Omega)F(\Omega) = b\Omega^2$.

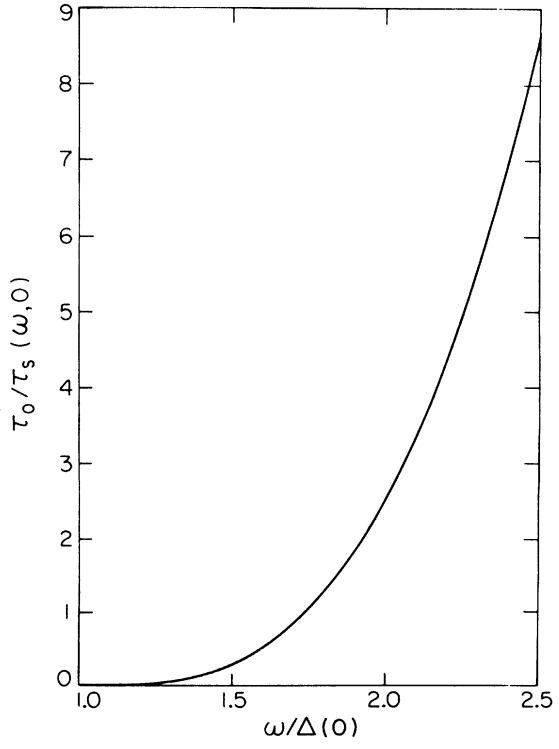

FIG. 3. Inverse scattering lifetime $\tau_s^{-1}(\omega, 0)$ at zero temperature vs the quasiparticle excitation energy. This curve is based upon the approximation $\alpha^2(\Omega)F(\Omega) = b\Omega^2$. τ_0 values for various metals are listed in Table I.

$$\tau_s^{-1}(\omega,0)=\frac{2\pi}{\hbar Z_1(0)}\int_0^{\omega-\Delta}d\Omega\,\alpha^2(\Omega)F(\Omega)\,\mathrm{Re}\left(\frac{\omega-\Omega}{[(\omega-\Omega)^2-\Delta^2]^{1/2}}\right)\left(1-\frac{\Delta^2}{\omega(\omega-\Omega)}\right), \tag{16}$$

where in this instance $\Delta=\Delta(0)$ everywhere. For $\alpha^2(\Omega)F(\Omega)=b\Omega^2$ this integral can be done[2] and one obtains

$$\tau_0/\tau_s^{-1}(\omega,0)=\left(\frac{\Delta}{kT_c}\right)^3\left(\frac{1}{3}\left[\left(\frac{\omega}{\Delta}\right)^2-1\right]^{3/2}+\frac{5}{2}\left[\left(\frac{\omega}{\Delta}\right)^2-1\right]^{1/2}-\frac{\Delta}{2\omega}\left[1+4\left(\frac{\omega}{\Delta}\right)^2\right]\ln\left\{\frac{\omega}{\Delta}+\left[\left(\frac{\omega}{\Delta}\right)^2-1\right]^{1/2}\right\}\right). \tag{17}$$

For ω larger than several times Δ, the scattering rate varies as $(\omega/\Delta)^3$. The curve in Fig. 3 shows a plot of $\tau_0/\tau_s(\omega,0)$ vs ω/Δ.

The recombination process is a binary reaction in which one quasiparticle combines with another to form a pair. Therefore, the recombination lifetime τ_r increases exponentially as $e^{\Delta(T)/kT}$ at low temperatures [Eq. (14)], reflecting the exponential decrease in the population of quasiparticles. The excess energy of the quasiparticles is emitted as a phonon. [We note that the recombination rate due to electron-electron interactions must go as $e^{-2\Delta(T)/kT}$ at low temperatures because here three quasiparticles are involved. This contribution is therefore negligible at sufficiently low temperatures.] As shown in Fig. 2, the recombination lifetime for a quasiparticle at the gap edge $[\omega=\Delta(T)]$ goes through a minimum value at a temperature slightly below T_c. In order to understand this, consider the recombination lifetime of a quasiparticle of energy ω. Because of the singularity in the quasiparticle density of states at the gap edge, it will tend to find a partner with energy $\Delta(T)$. Thus the resultant phonon emitted will have energy $\omega+\Delta(T)$. For $\omega=\Delta(T)$ (the top curve of Fig. 2) the emitted phonon energy is of order $2\Delta(T)$. As T increases from low temperatures, the quasiparticle population increases, and τ_r decreases as previously noted. However, for T/T_c greater than 0.9, $\tau_r(\Delta(T))$ goes through a minimum and then increases to its value at T_c. This is due to the fact that the phase space for low-energy phonons varies as Ω^2 so that as $2\Delta(T)$ goes to zero the rate for such a recombination goes to zero. The recombination of a quasiparticle with $\omega=\Delta(T)$ for $T\to T_c$ must then occur with a partner with an energy larger than the energy gap and hence a smaller quasiparticle density of states. This leads to the upturn of the $\omega=\Delta(T)$ curve as $T\to T_c$. For larger fixed values of ω, the curves do not have this feature.

As T approaches T_c, the limiting values of the lifetimes τ_s and τ_r for $\omega=\Delta(T_c)=0$ are equal as a consequence of particle-hole symmetry:

$$\tau_0/\tau_s(0,T_c)=\tau_0/\tau_r(0,T_c)=\tfrac{7}{4}\Gamma(3)\zeta(3)=4.20. \tag{18}$$

Physically this is simply a statement that, if there is particle-hole symmetry, a normal-state quasiparticle at the Fermi energy will have a rate of excitation by phonon absorption equal to its rate of excitation by phonon emission. The latter process, in which a phonon is emitted and the quasiparticle drops into an empty hole state below the Fermi surface, corresponds to *recombination* in the limit $T\to T_c$. It should be noted that our calculations are mean-field calculations and do not include fluctuations of the pair field which can become important for temperatures within the Ginsburg-Landau critical region near T_c.

It has been assumed by several authors[26,27] in developing simple models of the nonequilibrium state in superconductors that scattering is the dominant quasiparticle relaxation mechanism and that recombination processes form a bottleneck. From Fig. 4, one sees that, in thermal equilib-

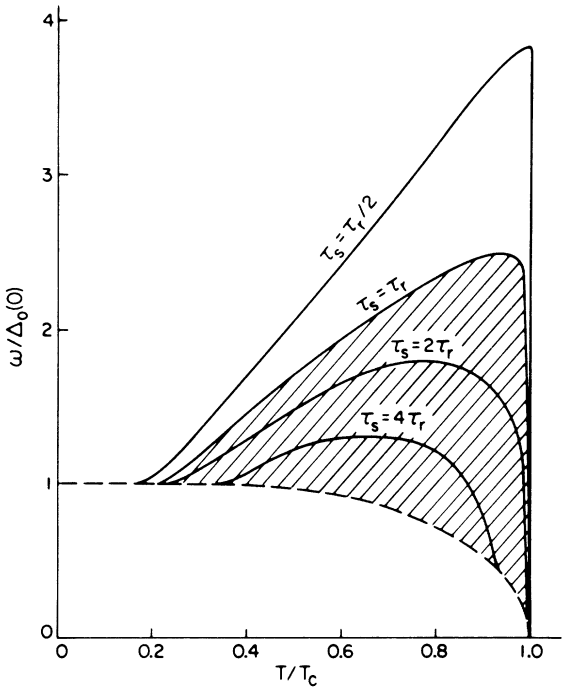

FIG. 4. Locus of points on the $\omega-T$ plane where $\tau_s=\frac{1}{2}\tau_r$, $\tau_s=\tau_r$, $\tau_s=2\tau_r$, and $\tau_s=4\tau_r$. The dashed line represents $\Delta(T)/\Delta(0)$, so that all quasiparticle states must lie above it. In the shaded region below the $\tau_s=\tau_r$ curve, the recombination lifetime τ_r is shorter than the scattering lifetime, while above this curve τ_s is shorter than τ_r. These curves were constructed using the universal $[\alpha^2(\Omega)F(\Omega)=b\Omega^2]$ results for τ_s and τ_r shown in Figs. 1 and 2.

rium, the scattering rate exceeds the recombination rate for quasiparticle states above the shaded region. However, for low-energy quasiparticles and temperatures above about $0.3T_c$, there is a substantial region where scattering is slower than recombination[27,28] and the simple nonequilibrium state theories are not adequate. In addition, for a nonequilibrium distribution with excess quasiparticles present the recombination rate will be increased further. For the strongly nonequilibrium state it would appear that a kinetic equation must be solved with the resulting distributions self-consistently used to determine the scattering rates.

For strong-coupling superconductors such as Pb and Hg with low-energy structure in $\alpha^2(\Omega)F(\Omega)$ it is necessary to use the complete tunneling data.[29] To illustrate this, $\alpha^2(\Omega)F(\Omega)$ and the low-frequency form $b\Omega^2$ for Pb are plotted in Fig. 5. The enlargement of the energy region 0–3 meV clearly shows the effect of the onset of umklapp processes above $\omega \sim 0.6$ meV. Figure 6 shows the integrand which enters in calculating τ_s^{-1} for $T/T_c = 0.44$. The dashed curve corresponds to the approximation $\alpha^2(\Omega)F(\Omega) = b\Omega^2$. The results for the scattering and recombination lifetimes for Pb and Hg using the complete tunneling data are shown in Figs. 7–9. The effect of using the exact $\alpha^2(\Omega)F(\Omega)$ spectrum is to shorten the lifetimes for Pb by about a factor of 2. In the case of Hg, a peculiar inversion of the $\tau_r(\omega, T)$ curves occurs at low temperatures; the higher-energy quasiparticles have longer recombination lifetimes than quasiparticles with lower energies. This arises from the fact that $\alpha^2(\Omega)F(\Omega)$ for Hg contains a large

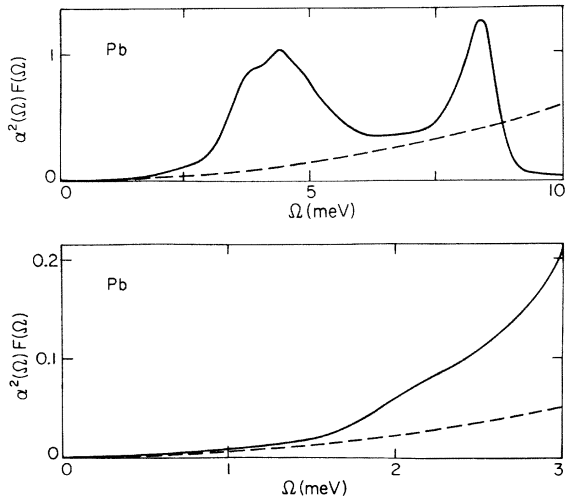

FIG. 5. Plot of $\alpha^2(\Omega)F(\Omega)$ (solid) and $b\Omega$ (dashed) vs Ω for Pb. The lower part shows an enlargement of the low-frequency region.

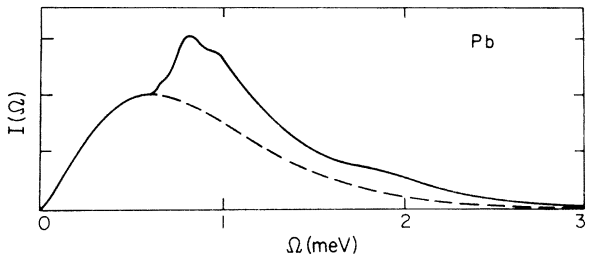

FIG. 6. Integrand $I(\Omega) \sim n(\Omega)\Omega^{1/2}\alpha^2(\Omega)F(\Omega)$ vs Ω for Pb at $T/T_c = 0.44$. This is the integrand which enters in calculating τ_s^{-1}. The solid curve is for the full $\alpha^2(\Omega)F(\Omega)$ while the dashed curve corresponds to approximating $\alpha^2(\Omega)F(\Omega)$ by $b\Omega^2$.

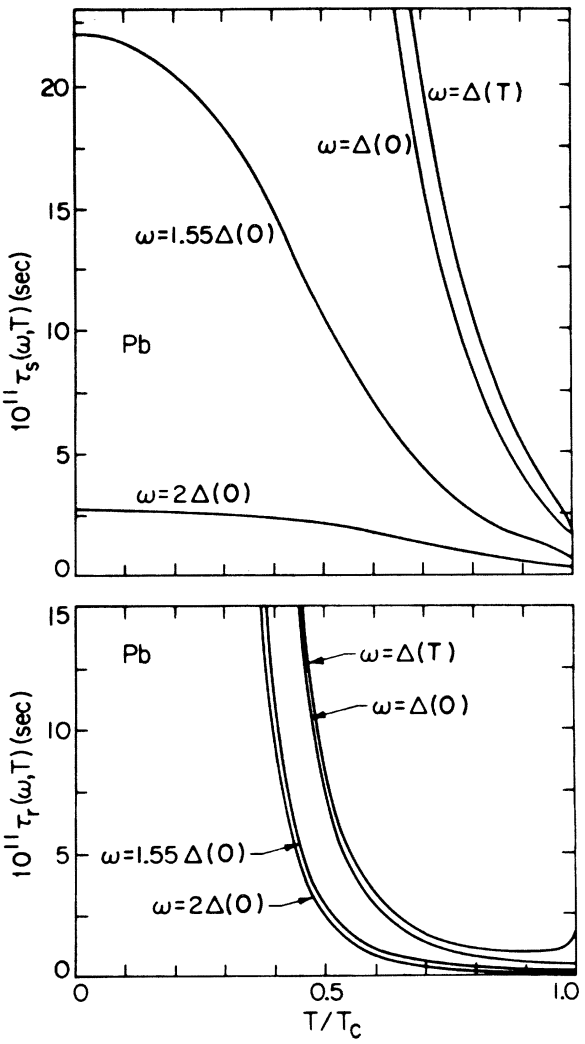

FIG. 7. Scattering τ_s and recombination τ_r lifetimes for Pb vs T/T_c for quasiparticles with excitation energy ω. The full $\alpha^2(\Omega)F(\Omega)$ tunneling data were used in the numerical integrations.

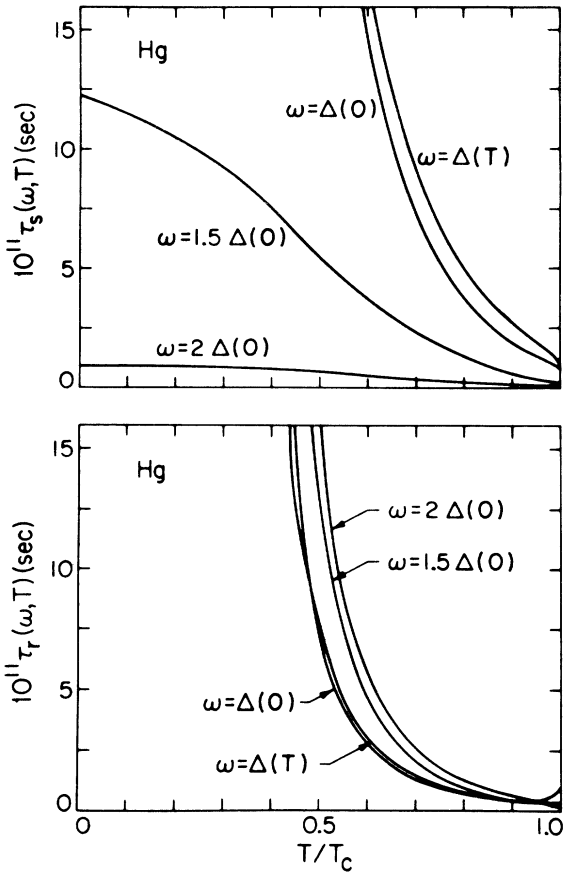

FIG. 8. Scattering τ_s and recombination τ_r lifetimes for Hg vs T/T_c for quasiparticles with excitation energy ω. The full $\alpha^2(\Omega)F(\Omega)$ tunneling data were used in the numerical integrations.

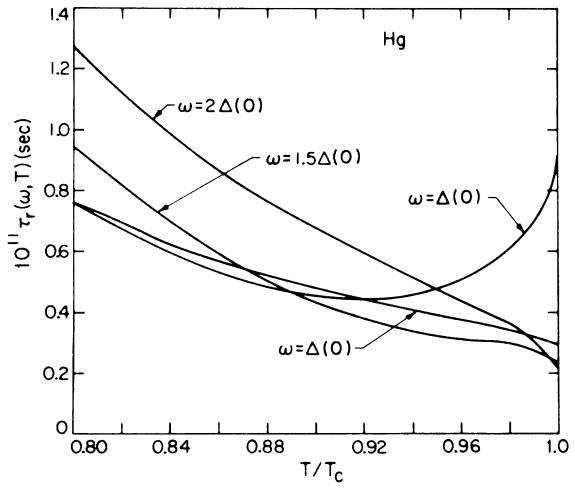

FIG. 9. Enlarged graph of τ_r for Hg vs T/T_c for T/T_c near 1.

low-frequency peak at $\Omega = 1.8$ meV. The gap for Hg is $\Delta(0) = 0.83$ meV, so that at low temperature the recombination of a quasiparticle with energy $\omega = \Delta(0)$ can occur with phonon emission which extends from $2\Delta(0) = 1.66$ meV on upwards including the peak, while a quasiparticle with energy $1.5\Delta(0)$ starts from $2.5\Delta(0) = 2.07$ meV and misses the peak. As T approaches T_c, the τ_r curve for $\omega = \Delta(T)$ eventually turns up because of the decrease in phonon phase space as previously discussed. Competing effects of the quasiparticle density of states and the low-lying peak in $\alpha^2(\Omega)F(\Omega)$ lead to the complicated crossings shown in detail in Fig. 9.

In Fig. 10, results for the zero-temperature scattering rate $\tau_s^{-1}(\omega, 0)$ are plotted for Pb and Hg. These were obtained by substituting the values of $Z(\omega)$ and $\Delta(\omega)$ computed directly from the tunneling I-V data[9] into Eq. (4) to obtain $\Gamma(\omega)$. At zero temperature, $\tau_s^{-1}(\omega, 0) = 2\Gamma(\omega)$. Over the energy region $\Delta < \omega \leq 3\Delta$, the values of $\tau_s^{-1}(\omega, 0)$ computed in this manner differ by as much as 30% at the higher-frequency end from the zero-temperature limiting values given in Figs. 7 and 8. This difference arises from two sources: (i) the values of $\Delta(\omega)$ given in Ref. 9 were computed using the

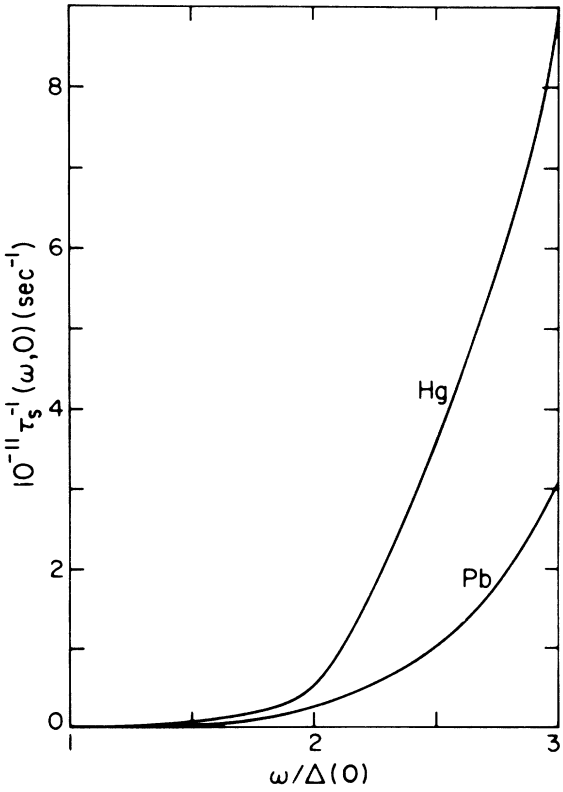

FIG. 10. Zero-temperature scattering rates $\tau_s^{-1}(\omega, 0)$ for Pb and Hg using the full $\alpha^2(\Omega)F(\Omega)$ data, vs ω.

Eliashberg equations with the frequency dependence of $\Delta(\omega, T)$ kept in the integrand rather than approximated by $\Delta(T)$ as we have done; (ii) the full frequency dependences of $Z_1(\omega)$ and $\phi_1(\omega)$ which appear in Eq. (4) rather than the approximate form of Eq. (5) were kept in the results shown in Fig. 10. This error is largest for the strong-coupling superconductors such as Pb and Hg where $Z_1(\omega)$ and $\phi_1(\omega)$ can have significant ω variation even over the region $\Delta \leq \omega \leq 3\Delta$. There are two additional possible sources for error: (i) the uncertainty in the low-frequency form of $\alpha^2(\Omega)F(\Omega)$; (ii) The quasiparticle approximation, which is essential in defining a lifetime, is only an approximation. We have discussed in Sec. II the rationale for using the Ω^2 fit to $\alpha^2(\Omega)F(\Omega)$ for small Ω. The quasiparticle approximation is known to fail as the quasiparticle energies approach the energies of the phonon peaks in $\alpha^2(\Omega)F(\Omega)$. However, at low energies, the quality factor Q of the quasiparticle resonance can be estimated in terms of the ratio of the quasiparticle energy to the energy width $\hbar/\tau$, where τ is the quasiparticle lifetime. A large Q value implies a narrow resonance. From Fig. 10 we note that for Pb, $Q(\omega = 2\Delta)$ is of order 10^2, while it drops to about 10 for $\omega = 3\Delta$. For comparison at finite temperatures, consider $\omega = \Delta(0)$ and $T/T_c = 0.9$. Then, using $\hbar(\tau_s^{-1} + \tau_r^{-1})$ as the width, one finds for Pb from Fig. 7 that Q is of order 10. A Q of 10 could lead to uncertainties of order 10%. For the more weakly coupled superconductors the Q is very large in this low-frequency region, and the quasiparticle approximation is excellent.

IV. BRANCH-MIXING TIME

In thermal equilibrium, the branches of the quasiparticle excitation curve corresponding to quasiparticle wave vectors less than and greater than the Fermi wave vector are equally occupied. There are situations, however, in which the branch populations are not necessarily equal, e.g., current flow across a supernormal interface,[30,31] or injection of quasiparticles into a superconductor through a tunnel barrier.[12-15] In such situations, we may distinguish among the inelastic processes we have been considering those which contribute to relaxation of the branch population imbalance. The associated lifetime is called the branch-mixing time τ_Q.[12-15] In this section we calculate the branch-mixing rate due to inelastic processes. Tinkham and Clarke[13,14] have pointed out that elastic processes can also contribute to branch mixing when there is a gap anisotropy or a spatially varying order parameter. We do not consider such processes here.

The $\chi\tau_3$ part of the Nambu self-energy[17] contributes to the scattering of a quasiparticle from one branch to another. Proceeding in a manner similar to that discussed in Sec. II, but keeping the $\chi\tau_3$ term, the quasiparticle branch-mixing lifetime τ_Q is

$$\tau_Q^{-1}(\omega) = \omega \frac{Z_2(\omega)}{Z_1} - \frac{\Delta}{\omega}\frac{\phi_2}{Z_1} + \frac{(\omega^2 - \Delta^2)^{1/2}}{\omega}\frac{\chi_2}{Z_1}, \tag{19}$$

with

$$\chi_2(\omega) = -\pi \int_0^{\omega-\Delta} d\Omega\, \alpha^2(\Omega)F(\Omega)[f(\Omega-\omega)+n(\Omega)] - \pi \int_{\omega+\Delta}^{\infty} d\Omega\, \alpha^2(\Omega)F(\Omega)[f(\Omega-\omega)+n(\Omega)]$$
$$+\pi \int_0^{\infty} d\Omega\, \alpha^2(\Omega)F(\Omega)[f(\omega+\Omega)+n(\Omega)]\,. \tag{20}$$

Here we have kept those processes which scatter a quasiparticle from one branch to the other as well as those recombination or pair-breaking processes which involve two quasiparticles on the same branch. Combining the terms in Eq. (19) and changing variables, one can write $\tau_Q^{-1}(\omega)$ in the more transparent form

$$\tau_Q^{-1}(\omega) = \frac{\pi}{\hbar Z_1(0)}\frac{1}{1-f(\omega)}\Bigg[\int_0^{\epsilon} d\epsilon'\, \alpha^2(\omega-\omega')F(\omega-\omega')[n(\omega-\omega')+1][1-f(\omega')]\left(1-\frac{\Delta^2+\epsilon\epsilon'}{\omega\omega'}\right)$$
$$+\int_{\epsilon}^{\infty} d\epsilon'\, \alpha^2(\omega'-\omega)F(\omega'-\omega)n(\omega'-\omega)[1-f(\omega')]\left(1-\frac{\Delta^2+\epsilon\epsilon'}{\omega\omega'}\right)$$
$$+\int_0^{\infty} d\epsilon'\, \alpha^2(\omega+\omega')F(\omega+\omega')[n(\omega+\omega')+1]f(\omega')\left(1+\frac{\Delta^2-\epsilon\epsilon'}{\omega\omega'}\right)\Bigg]. \tag{21}$$

Here $\omega' = (\epsilon'^2+\Delta^2)^{1/2}$ and $\epsilon = (\omega^2-\Delta^2)^{1/2}$. The first term in Eq. (21) corresponds to the scattering of a quasiparticle of energy ω on one branch to a state of lower energy ω' on the other branch with the emission of a phonon of energy $\omega - \omega'$. The second term represents a scattering with the absorption of a phonon. The last term is the contribution from the recombination of a quasiparticle of energy ω with another quasiparticle from the same branch. Equation (21) differs from Eq. (8) in the

appearance of the term $\epsilon\epsilon'/\omega\omega'$ in each coherence factor. This term vanishes by symmetry when inelastic processes involving scattering to both branches are allowed. This branch restriction also accounts for the factor of 2 difference between Eq. (21) and Eq. (8).

Figure 11 presents results calculated from Eq. (21) using the quadratic approximation $\alpha^2(\Omega)F(\Omega) = b\Omega^2$ and the BCS relation $2\Delta = 3.52kT_c$. τ_0 is the characteristic unit time defined in Eq. (10).

For energies $\omega \gg \Delta(T)$, a useful approximate form for τ_Q is

$$\tau_0\tau_Q^{-1}(\omega, T) \cong \frac{1}{2}\frac{\Delta(T)}{\Delta(0)}\left(\frac{\omega}{kT_c}\right)^2\left(\frac{\Delta(0)}{kT_c}\right)\coth\left(\frac{\omega}{2kT}\right). \tag{22}$$

If the identification $\alpha^{-1} = \tau_0(kT_c)^3$ is made, where α is the constant used in Refs. 13 and 14, we see that Eq. (22) is just the result obtained by Tinkham and Clarke except that it is half as large.[32] This results simply from a difference in definition of τ_Q: Tinkham and Clarke's τ_Q^{-1} is the rate at which the branch imbalance $Q = n_> - n_<$ changes ($n_>$ and $n_<$ are the numbers of quasiparticles on the $k > k_F$ and $k < k_F$ branches). Our τ_Q^{-1} is the rate at which f_k changes. In a single branch-mixing event, Q changes by two while f_k changes by one. Our τ_Q^{-1} is thus just half Tinkham and Clarke's. The experimentally observed[12,15] divergence of τ_Q as $\Delta^{-1}(T)$ for $T \to T_c$ is apparent in Eq. (22).

For $T = 0$, we find

$$\tau_0\tau_Q^{-1}(\omega, 0) = \frac{1}{2(kT_c)^3}\left[[\omega^2 - \Delta^2(0)]^{1/2}\left(\tfrac{1}{3}[\omega^2 - \Delta^2(0)] + \tfrac{5}{2}\Delta^2(0) - \frac{[\omega - \Delta(0)]^3}{3\omega}\right)\right.$$
$$\left. - \left(2\omega\Delta^2(0) + \frac{\Delta^4(0)}{2\omega}\right)\ln\left(\frac{[\omega^2 - \Delta^2(0)]^{1/2} + \omega}{\Delta(0)}\right)\right]. \tag{23}$$

If $\omega \gg \Delta(0)$, Eq. (23) reduces essentially to the low-temperature limit obtained by Tinkham and Clarke.[13,14] However, their result differs from Eq. (23) for energies just above the gap and, in particular, does not predict the low-temperature increase in τ_Q shown in Fig. 11 and evident in experimental data[15] (see Sec. VI).

It follows from Eqs. (21) and (8) that $\tau_Q^{-1} \leq \frac{1}{2}(\tau_s^{-1} + \tau_r^{-1})$, the average of the quasiparticle scattering and recombination rates. The equality holds at the gap edge, $\omega = \Delta(T)$ (where, however, quasiparticle scattering events cannot strictly be called branch-mixing events). This leads to a nonzero limiting value for $\tau_Q^{-1}(\Delta(T))$ at $T = T_c$ given by $\tau_0\tau_Q^{-1}(\Delta(T), T_c) = \frac{7}{4}\Gamma(3)\zeta(3)$, whereas, for quasiparticles with energies greater than Δ, τ_Q^{-1} goes to zero as $\Delta(T)$ when $T \to T_c$ and τ_Q therefore diverges. Figure 12 provides a means of visualizing the way in which these different limits are approached as well as a generally useful way to visualize the energy and temperature dependence of the characteristic quasiparticle times. It shows three-dimensional sketches of the rates τ_s^{-1}, τ_r^{-1}, and τ_Q^{-1} as a function of ω and T. The rather peculiar ordering of the τ_Q curves near T_c which is apparent in Fig. 11 is associated with the "saddle" in this region in Fig. 12(c). It is caused by minima in both the scattering and recombination contributions to τ_Q^{-1} which arise from the $\epsilon\epsilon'/\omega\omega'$ terms in the coherence factors in Eq. (21).

In the calculation of τ_Q for Pb and Hg it is again necessary to use the full $\alpha^2(\Omega)F(\Omega)$ function rather than the quadratic approximation. The results for these superconductors are shown in Figs. 13 and 14. The rather complex structure and crossings in the Hg curves result from the prominent low-energy structure in $\alpha^2(\Omega)F(\Omega)$ for Hg.

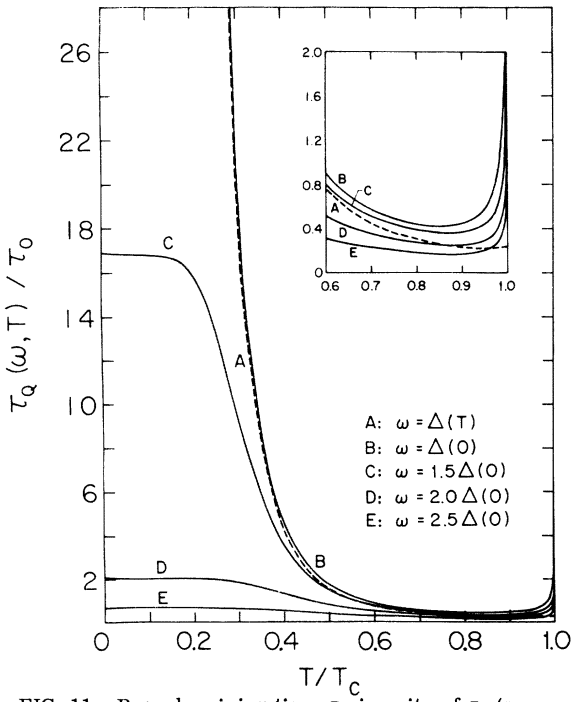

FIG. 11. Branch-mixing time τ_Q in units of τ_0 (see Table I) vs T/T_c for quasiparticles with various excitation energies E. The inset shows an enlargement of the vertical scale for temperatures near T_c. For these curves $\alpha^2(\Omega)F(\Omega) = b\Omega^2$.

V. PHONON LIFETIMES

In this section we calculate the lifetimes of a phonon against Cooper pair-breaking $\tau_B(\Omega, T)$ and against scattering with a quasiparticle $\tau_{phs}(\Omega, T)$. These characteristic phonon times are of interest in connection with nonequilibrium situations in superconductors in which phonon-trapping effects are important[1] and in the application of superconductors to the generation and detection of ultrahigh-frequency phonons. A number of authors[33-35] have carried out this type of calculation in determining the ultrasonic attenuation. Here, follow-

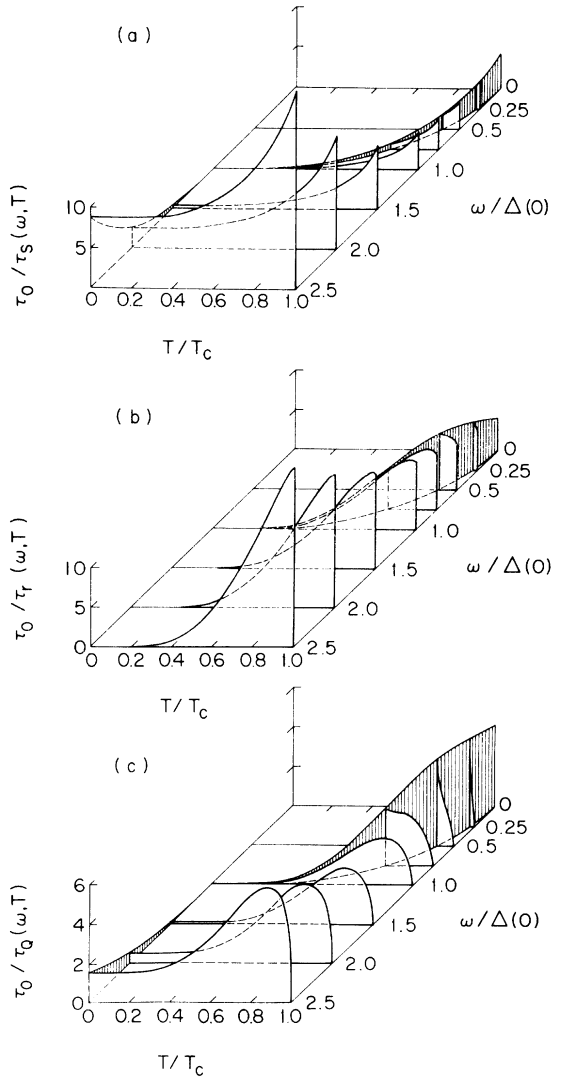

FIG. 12. Perspective views of the energy and temperature dependence of the quasiparticle scattering rate (a), recombination rate (b), and branch-mixing rate (c). The vertically shaded wall at the rear of each figure represents the trace of the appropriate rate on the surface $\Delta(T)$.

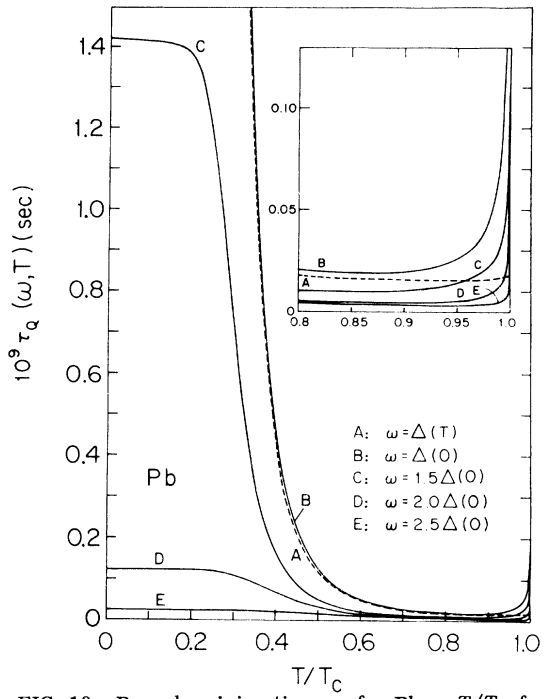

FIG. 13. Branch-mixing time τ_Q for Pb vs T/T_c for quasiparticles with various excitation energies ω. The inset shows an enlargement of the high-temperature region. The full $\alpha^2(\Omega)F(\Omega)$ tunneling data were used in the numerical integrations.

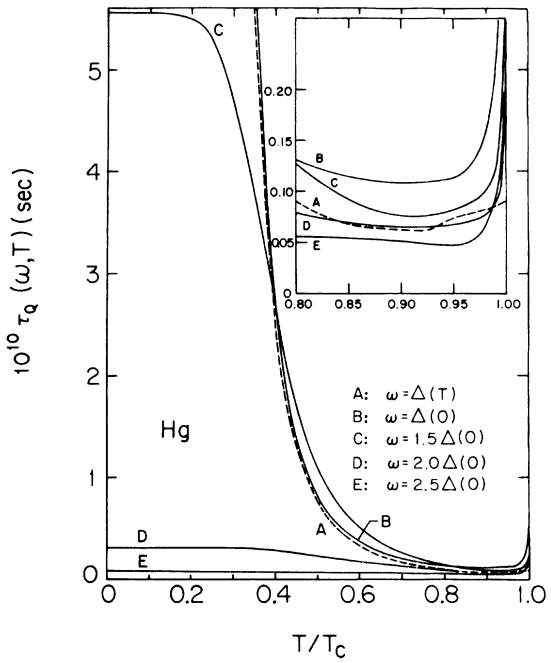

FIG. 14. Branch-mixing time τ_Q for Hg vs T/T_c for quasiparticles with various excitation energies ω. The inset shows an enlargement of the high-temperature region. The full $\alpha^2(\Omega)F(\Omega)$ tunneling data were used in the numerical integrations.

ing a brief review of the formalism, we give some results for phonon lifetimes. These can be obtained from various published work and are included here for completeness.

We employ the Green's-function techniques which lead to the Eliashberg formalism used in Sec. II. The poles of the phonon Green's function are determined by

$$\Omega^2 - \Omega_{\vec{q}\lambda}^2 - 2\Omega_{\vec{q}\lambda}\pi_\lambda(\vec{q},\Omega)\left|g_\lambda(\vec{q})\right|^2/\epsilon(\vec{q},\Omega) = 0\,, \quad (24)$$

where $\pi_\lambda(\vec{q},\Omega)$ is the irreducible polarization, $g_\lambda(\vec{q})$ is the electron-phonon matrix element, and $\epsilon(\vec{q},\Omega)$ is the Coulomb dielectric constant. Setting $\Omega = \omega_{\vec{q}\lambda} - i\gamma$ and assuming that imaginary parts are small compared with real parts, Eq. (24) yields

$$\gamma = -(\Omega_{q\lambda}/\omega_{q\lambda})\left|g_\lambda(\vec{q})\right|^2 \times \mathrm{Im}[\,\pi_\lambda(\vec{q},\omega_{\vec{q}\lambda})/\epsilon(\vec{q},\omega_{\vec{q}\lambda})]\,. \quad (25)$$

The inverse phonon lifetime τ_{ph}^{-1} is equal to 2γ. The taking of the imaginary part of the bracketed expression in Eq. (25) yields the imaginary part of π_λ times the factor $|\epsilon(\vec{q},\omega_{\vec{q}\lambda})|^{-2}$. We note that $\epsilon_2 \ll \epsilon_1$ at these energies, and absorb $[\,\epsilon(q,\omega_{\vec{q}\lambda})]^{-2}$ with the factor $\Omega_{\vec{q}\lambda}/\omega_{\vec{q}\lambda}$ into $|g_\lambda(\vec{q})|^2$ to obtain the *effective* electron-phonon matrix element[17] $\bar{g}_\lambda(\vec{q})$ which enters in the definition of $\alpha^2(\Omega)F(\Omega)$. In the same spirit as the Eliashberg calculation of the quasiparticle self-energy discussed in Sec. II, π_λ is approximated by the usual bubble graph. Just as in the discussion of quasiparticles, it is useful to consider the average lifetime of a phonon of a particular energy Ω. We therefore define $\pi(\Omega)$ by

$$\pi(\Omega) = \sum_{\vec{q}\lambda}\delta(\Omega - \omega_{\vec{q}\lambda})\pi_\lambda(\vec{q},\omega_{\vec{q}\lambda}) \Big/ \sum_{\vec{q}\lambda}\delta(\Omega - \omega_{\vec{q}\lambda}) = \sum_{\vec{q}\lambda}\delta(\Omega - \omega_{\vec{q}\lambda})\pi_\lambda(\vec{q},\omega_{\vec{q}\lambda}) \Big/ NF(\Omega)\,, \quad (26)$$

where N is the ion number density and $F(\Omega)$ is the phonon density of states $[\int F(\Omega)\,d\Omega = 3]$. In addition, we make use of the definition of $\alpha^2(\Omega)F(\Omega)$, Eq. (3). We can then eliminate $|\bar{g}_\lambda(\vec{q})|^2$ in favor of $\alpha^2(\Omega)$. This leads to an average of the phonon inverse lifetime over the polarization and direction of $\vec{q}$ which is proportional to $\alpha^2(\Omega)$. We believe that this average is the one appropriate to the dirty superconductor we are considering here.

The phonon decay rate is separable into two parts which can be recognized by their coherence factors. The pair-breaking rate τ_B^{-1} contains the same coherence factor as the quasiparticle recombination lifetime; the quasiparticle and phonon scattering rates τ_s^{-1} and τ_{phs}^{-1} contain common factors as well [see Eq. (6)]. These times are given by

$$\tau_B^{-1}(\Omega) = \frac{4\pi N(0)\alpha^2(\Omega)}{\hbar N}\int_\Delta^{\Omega-\Delta}\frac{d\omega}{(\omega^2-\Delta^2)^{1/2}}\,\frac{\omega(\Omega-\omega)+\Delta^2}{[(\Omega-\omega)^2-\Delta^2]^{1/2}}\,[1 - f(\omega) - f(\Omega-\omega)]\,, \quad (27)$$

$$\tau_{phs}^{-1}(\Omega) = \frac{8\pi N(0)\alpha^2(\Omega)}{\hbar N}\int_\Delta^{\infty}\frac{d\omega}{(\omega^2-\Delta^2)^{1/2}}\,\frac{\omega(\Omega+\omega)-\Delta^2}{[(\Omega+\omega)^2-\Delta^2]^{1/2}}\,[f(\omega) - f(\omega+\Omega)]\,. \quad (28)$$

Here $\tau_B(\Omega)$ is the lifetime of a phonon of energy Ω due to absorption with pair breaking and $\tau_{phs}(\Omega)$ is the scattering lifetime of a phonon of energy Ω. $N(0)$ is the single-spin band-structure electronic density of states at the Fermi surface and does not include electron-phonon renormalization effects. These expressions for the lifetimes can also be obtained using the golden rule.

In order to determine τ_B and τ_{phs}, we need $\alpha^2(\Omega)$. In principle this can be obtained by using neutron scattering data to find $F(\Omega)$ and then dividing this $F(\Omega)$ out of the $\alpha^2(\Omega)F(\Omega)$ obtained from tunneling experiments. $F(\Omega)$ at low energies can also be obtained from a fit to the Debye model using experimental Debye temperatures. Estimates of $\alpha^2(\Omega)$ using a Debye model are given in Table II, along with values of $\alpha^2(2\Delta(0))$ for three superconductors obtained from neutron scattering and tunneling data.

For purposes of plotting universal curves for τ_B and τ_{phs} we define an average $\alpha^2(\Omega)$ by

$$3\langle\alpha^2\rangle_{av} \equiv \int_0^\infty \alpha^2(\Omega)F(\Omega)\,d\Omega\,. \quad (29)$$

The area of the $\alpha^2(\Omega)F(\Omega)$ spectrum is given in Ref. 7 for all but three of the superconductors listed in Table I. For Al and Zn we have made use of theoretical calculations[24,25] of $\alpha^2(\Omega)F(\Omega)$ to find $\langle\alpha^2\rangle_{av}$. For Nb, neutron data were used.[22] We define a characteristic time τ_0^{ph} by

$$\tau_0^{ph} \equiv \hbar N/4\pi^2 N(0)\langle\alpha^2\rangle_{av}\Delta(0)\,. \quad (30)$$

Values of τ_0^{ph} for several superconductors are listed in Table II. Figures 15 and 16 show results for $\tau_0^{ph}\tau_B^{-1}$ and $\tau_0^{ph}\tau_{phs}^{-1}$ calculated from Eqs. (27) and (28). Figure 15 shows the temperature dependence of these inverse lifetimes at energies which are multiples of $\Delta(T)$, and Fig. 16 shows them at constant energies. We have assumed the BCS relation $2\Delta(0) = 3.52kT_c$ in calculating these curves.

In the limit $\Omega \ll kT$, $\Delta(T)$, we arrive at the familiar relation for the acoustic attenuation of

TABLE II. Characteristic phonon times and associated parameters.

Metal	$N(0)$ [a] (10^{21} states/eV)	N [a] (10^{22} ions/cm^3)	$\langle\alpha^2\rangle_{av}$ (meV)	α_D^2 [b] (meV)	$\alpha^2(2\Delta(0))$ [c] (meV)	τ_0^{ph} (10^{-10} sec)
Pb	8.63	3.30	1.34	0.473	1.3	0.340
In	7.68	3.84	0.913	0.842		1.69
Sn	8.14	3.70	1.14	1.31		1.10
Hg	7.26	4.07	0.833	2.07		1.35
Tl	11.7	3.50	0.666	0.454		2.05
Ta	40.8	3.52	1.38	1.71	2.55	0.227
Nb	31.7	5.57	4.6	5.92	4.0	0.0417
Al	12.2	6.02	1.93	1.77	1.99	2.42
Zn	6.64	6.57	0.596	1.05		23.1

[a] Data on the normal state properties were taken from Ref. 23.

[b] These are estimates of α^2 using a Debye model for $F(\Omega)$ and the $b\Omega^2$ form for $\alpha^2(\Omega)F(\Omega)$. $\alpha_D^2=\alpha^2(\Omega)F(\Omega)/F(\Omega)=\frac{1}{9}b(k\Theta_D)^3$. Θ_D is found in Ref. 36. One must be careful in applying these numbers: For instance, at low temperatures $\alpha^2(\Omega)F(\Omega)$ for Pb is no longer quadratic at $\Omega=2\Delta(0)$. If one uses the actual tunneling data at this energy and notes that $F(\Omega)$ is still quadratic there, $\alpha_D^2(2\Delta(0))=1.63$, in fairly good agreement with the other values for this metal.

[c] The neutron data for $F(\Omega)$ for Pb (Ref. 37), Ta (Ref. 38), and Al (Ref. 37) were used to estimate $\alpha^2(2\Delta(0))$ by comparing with $\alpha^2(\Omega)F(\Omega)$ at this energy. By using an average value of $\lambda=1.84$ (Ref. 23), a crude estimate of $\alpha^2(\Omega)F(\Omega)$ was made for Nb using the neutron data of Ref. 22. The value of $\alpha^2(2\Delta(0))$ was obtained from this estimate.

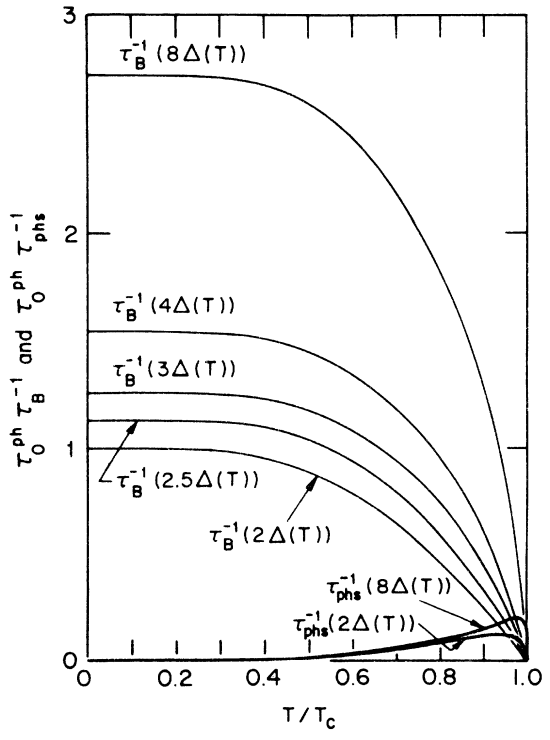

FIG. 15. Phonon pair-breaking rate $\tau_B^{-1}(\Omega,T)$ in units of $(\tau_0^{ph})^{-1}$ and the phonon scattering rate $\tau_{phs}^{-1}(\Omega,T)$ in units of $(\tau_0^{ph})^{-1}$, vs T/T_c. The phonon energies Ω in this plot are multiples of the gap energy $\Delta(T)$. τ_0^{ph} for various materials is given in Table II.

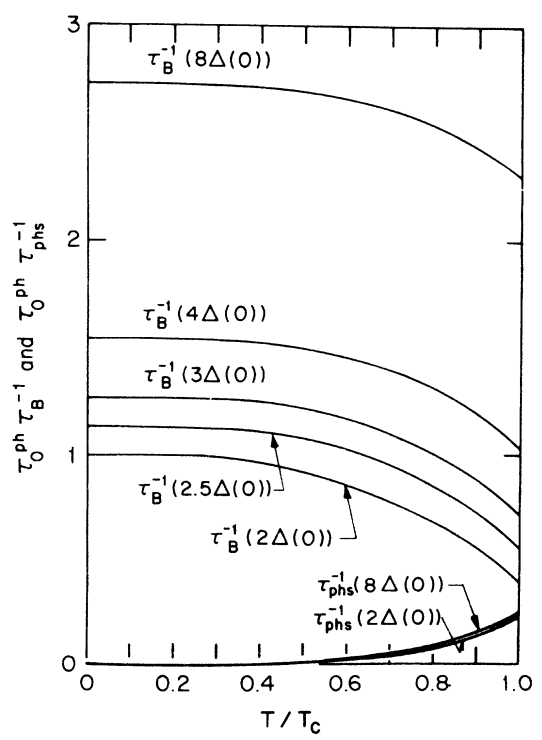

FIG. 16. Phonon pair-breaking rate $\tau_B^{-1}(\Omega,T)$ in units of $(\tau_0^{ph})^{-1}$ and the phonon scattering rate $\tau_{phs}^{-1}(\Omega,T)$ in units of $(\tau_0^{ph})^{-1}$, vs T/T_c. The phonon energies Ω are constants in this plot. τ_0^{ph} for various materials is given in Table II.

a low-frequency phonon

$$\tau_0^{ph}\tau_{phs}^{-1}(\Omega, T) = [2\Omega/\pi\Delta(0)]f(\Delta(T)) \ . \quad (31)$$

In the low-temperature limit and for $\Omega \ll \Delta(T)$, the leading behavior of Eq. (28) is

$$\tau_0^{ph}\tau_{phs}^{-1}(\Omega, T) = [2kT/\pi\Delta(0)]e^{-\Delta(T)/kT}(1 - e^{-\Omega/kT}) \ . \quad (32)$$

The first exponential function in Eq. (32) reflects the number of quasiparticles available for scattering, which is small at low temperatures.

The pair-breaking rate at the threshold energy $\Omega = 2\Delta(T)$ is

$$\tau_0^{ph}\tau_B^{-1}(2\Delta(T)) = [\Delta(T)/\Delta(0)][1 - 2f(\Delta(T))] \ . \quad (33)$$

The thermal factors reflect the number of pairs available for pair breaking, which explains why in Fig. 15 the scattering rate does not begin to approach the pair-breaking rate at the gap edge until T approaches T_c. Figure 16 shows that the scattering rate at constant phonon energy is less than the corresponding pair-breaking rate for all temperatures, and at T_c is only about half the pair-breaking rate for a phonon of energy $2\Delta(0)$. Since we believe that no other inelastic scattering processes would yield a rate comparable to that of pair breaking, the mean free path of a phonon of energy greater than the energy gap is controlled by the pair-breaking time for $T \lesssim 0.9T_c$.

At T_c, the integrals in Eqs. (27) and (28) can be evaluated analytically and yield

$$\tau_0^{ph}\tau_{phs}^{-1}(\Omega, T_c) = \frac{2kT_c}{\pi\Delta(0)} \ln\left(\frac{2}{1+\exp(-\Omega/kT_c)}\right) , \quad (34)$$

$$\tau_0^{ph}\tau_B^{-1}(\Omega, T_c) = \Omega/\pi\Delta(0) - \tau_0^{ph}\tau_{phs}^{-1}(\Omega, T_c) \ . \quad (35)$$

Unlike the quasiparticle lifetimes, the phonon lifetimes are not equal at T_c because they represent different processes in the normal state. The "pair-breaking" process above T_c represents the excitation of an electron across the Fermi surface, while the scattering rate is merely electron-phonon scattering where the electron does not cross the Fermi surface. The total inverse lifetime at T_c is shown by Eq. (35) to be proportional to the phonon energy.

VI. COMPARISON OF THEORY WITH EXPERIMENT

A. Nuclear-spin-relaxation rate

It is well known that the original BCS theory predicted that the nuclear-spin-relaxation rate in a superconductor diverges as $\ln|T_c/(T_c - T)|$ as T approaches T_c from below.[39] Fibich[40] showed that when quasiparticle lifetime effects are taken into account, the divergence is cut off and the argument of the logarithm becomes $|4\Delta/\Delta_2(\Delta)|$, where $\Delta_2(\Delta)$ is the imaginary part of $\Delta(\omega)$ for $\omega = \Delta(T)$, and $\Delta = \Delta(T)$. This can be expressed in terms of the total quasiparticle lifetime $\tau = (\tau_s^{-1} + \tau_r^{-1})^{-1}$ for a quasiparticle with energy $\omega = \Delta(T)$ (i.e., a quasiparticle at the gap edge):

$$|\Delta/\Delta_2(\Delta)| = 2\Delta\tau(\Delta)/\hbar \quad (36)$$

is just the Q of the gap-edge quasiparticle resonance. Figure 17 gives a universal plot of $|\Delta_2(\Delta)/\Delta|$ as a function of reduced temperature

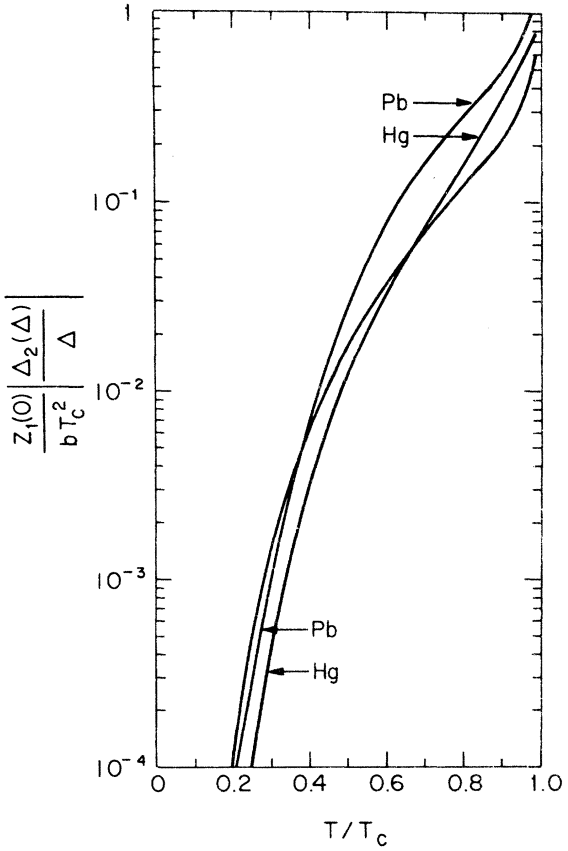

FIG. 17. Ratio of imaginary and real parts of the gap parameter (inverse Q of the gap-edge quasiparticle resonance) as a function of temperature. $|\Delta_2(\Delta)/\Delta|$ for a particular superconductor can be obtained by applying the indicated parameters from Table I; b is in units of meV^{-2}. The unlabeled curve is a universal curve for cases where $\alpha^2(\Omega)F(\Omega) = b\Omega^2$ is a good approximation. The curves for Hg and Pb were derived from our calculations based on the actual $\alpha^2(\Omega)F(\Omega)$ functions for these superconductors. In deriving these curves, we have assumed that the BCS temperature dependence (Ref. 41) for $\Delta(T)/\Delta$ is adequate for all cases, and that $2\Delta(0) = akT_c$. For the universal curve we have taken the BCS value, $a = 3.52$. Here and elsewhere in our calculations we have taken $a = 4.3$ for Pb (Ref. 42) and $a = 4.6$ for Hg (Ref. 43).

together with specific curves for Pb and Hg, all calculated from our previous results.

Comparison of our results with experimental measurements of the nuclear-spin-relaxation rate is complicated by the fact that anisotropy and spatial inhomogeneity of the gap can also cut off the logarithmic divergence. For Al, Fibich's formula and our results predict that the maximum in the spin-relaxation rate (which occurs at $T/T_c \cong 0.8$) should be a factor of 5.5 larger than the normal-state rate at the same temperature. The experimental data[39,44,45] indicate a maximum relation rate enhancement factor of about 2.2. This discrepancy can be attributed to gap anisotropy[39] which, although relatively small in Al, nevertheless seems to dominate lifetime broadening effects in this material.

For In, our results predict a maximum relaxation rate enhancement factor of 3.2. The factor experimentally observed[39,46] in an In–1.02-at.%-Tl alloy (in which gap anisotropy should be substantially averaged out due to the short impurity-limited electronic mean free path) is about 2.5. The agreement between theory and experiment is thus considerably better for In than for Al. Williamson[46] and MacLaughlin[39] compared their experimental In results with theory using a $\Delta_2(\Delta)/\Delta$ function calculated from the theory of Scalapino and Wu[47] (see Fig. 9 of Ref. 39). They noted "a serious discrepancy, especially at low temperatures."[39] Our $\Delta_2(\Delta)/\Delta$ function is approximately a factor 3.3 larger than Williamson and MacLaughlin's in the region of the relaxation-rate maximum but falls off more rapidly with decreasing temperature. The reason for this difference is unclear, but it seems likely that the use of our function in a detailed comparison with experiment might reduce the discrepancy.

Despite the large amount of experimental work which has been done on nuclear-spin relaxation in superconductors, there appear to be no other such data with which a useful comparison of our theoretical results can be made.

B. Riedel singularity in the Josephson supercurrent amplitude

Another characteristic logarithmic singularity resulting from the singularity in the BCS quasiparticle density of states occurs in the amplitude of the Josephson supercurrent[48] in superconducting tunnel junctions and is called the Riedel singularity.[49] Here again the singularity is cut off by the quasiparticle lifetime broadening effects,[47] leaving a $\pi^{-1} \ln|4\Delta/\Delta_2(\Delta)|$ enhancement of the supercurrent amplitude at the gap voltage $V_g = 2\Delta/e$. Unfortunately, here again anisotropy and spatial inhomogeneity of the gap can also contribute to truncation of the singularity.

Detailed experimental studies of the Riedel singularity have been made for Sn.[50-54] Buckner and Langenberg[52-54] compared their experimental results with an unpublished theoretical calculation of $\Delta_2(\Delta)/\Delta$ for Sn by Scalapino and Taylor[11] and found good agreement for $T/T_c \gtrsim 0.8$. At lower temperatures gap anisotropy appears to become the dominant factor limiting the Riedel singularity and the data can be quantitatively accounted for in terms of the known gap anisotropy of Sn.[54] The $\Delta_2(\Delta)/\Delta$ function calculated here is a factor of 1.7 larger at all temperatures than the Scalapino-Taylor result used by Buckner and Langenberg. The experimental uncertainties are such that the data cannot be said to favor definitely either theoretical result. Use of our present theoretical result would not materially change any of the conclusions of Buckner and Langenberg.

Vernet and Adde[55] have observed the Riedel peak in Ta-Ta point contacts. The applicability of theory developed for tunnel junctions to point contacts may be questioned, but Vernet and Adde argue that under their experimental conditions tunneling currents dominate in their point contacts. Analyzing their results using the Scalapino-Wu theory,[47,54] they find $\Delta_2(\Delta)/\Delta \sim 10^{-4}$ at $T/T_c = 0.9$. This is about a factor 40 smaller than our present theoretical value for Ta.

The Riedel peak has also been observed in point contacts (here Ta-Sn contacts) by Thomé and Couder.[56] They estimate $\Delta_2(\Delta)/\Delta < 4 \times 10^{-2}$ at an unspecified temperature. This upper limit is considerably larger than our theoretical estimates would suggest.

Kofoed and Saermark[57] have observed the Riedel peak in Sn and In weak links. Again using the Scalapino-Wu theory, they report a value of $\Delta_2(0)/\Delta \sim 10^{-3}$ for In, over the temperature range $T/T_c = 0.6$–0.9. This is several times smaller than our theoretical estimate in this temperature range.

The logarithmic dependence of the Riedel peak amplitude on $\Delta_2(\Delta)/\Delta$ makes measurements of this amplitude a rather poor source of experimental information on $\Delta_2(\Delta)/\Delta$ and probably accounts at least in part for the crudeness of the correspondence between our theoretical estimates and existing experimental results. About all that can confidently be said on this score is that theory and experiment are not in clear disagreement.

C. Quasiparticle current jump

A third singularity of interest is the jump in the quasiparticle current I_{qp} in a superconducting tunnel junction which occurs at the voltage V_g

$= 2\Delta/e$. The simplest theory of the tunnel current predicts that this jump should be a step discontinuity. As with the nuclear-spin-relaxation rate and Riedel singularities, quasiparticle lifetime effects and gap anisotropy or spatial inhomogeneity are expected to broaden the quasiparticle current jump singularity, leading to a finite slope $(dI_{qp}/dV)_{V=V_g}$. The contribution to this slope of a nonzero $|\Delta_2(\Delta)/\Delta|$ is[11]

$$\left(\frac{dI_{qp}}{dV}\right)_{V=V_g} = \frac{1}{4R_N}\left|\frac{\Delta}{\Delta_2(\Delta)}\right| \tanh\left(\frac{\Delta}{2kT}\right), \qquad (37)$$

where R_N is the normal-state tunnel junction resistance. Buckner and Langenberg[53,54] studied this "discontinuity" in the same tunnel junctions in which they studied the Riedel singularity, but were unable to account for the observed slope in terms of lifetime broadening and gap anisotropy effects, even though they were able to do so successfully for the Riedel singularity.

D. Quasiparticle recombination lifetime

The relative insensitivity of a logarithm to the value of its argument, together with the obscuring effects of gap anisotropy and spatial inhomogeneity, cause the above types of experiments to yield only rather crude tests of our calculations. Experimental data on quasiparticle recombination lifetimes should provide a much better test. Such data exist for three materials, Al, Sn, and Pb. Unfortunately, almost all quasiparticle-recombination-lifetime experiments to date appear to be complicated by a phonon-trapping effect[58] which makes difficult the extraction of an intrinsic quasiparticle recombination lifetime for comparison with our theoretical results.

The simplest way to compare experimental and theoretical recombination times is to compare the theoretical τ_0 with an experimental τ_0 derived from low-temperature recombination time data via Eq. (14). In doing so, it is necessary to take into account the fact that, with the exception of the Cambridge group,[7,59] experimentalists usually quote the decay time of an excess quasiparticle distribution while the results of theoretical calculations (the present one included) are quoted as the time associated with recombination of a given quasiparticle. Since *two* quasiparticles vanish in a single recombination event, most quoted experimental times must be multiplied by two before comparing them with theory.

We consider first the results of Gray *et al.*[7,59] for Al. For a three-film structure of total thickness ~900 Å on glass, in vacuum (denoted as vacuum–900-Å-Al–glass), they find $\tau_0(\text{expt}) = 4\times10^{-6}$ sec in a steady-state experiment and $\tau_0(\text{expt}) = 1.4\times10^{-6}$ sec in a transient experiment. For vacuum–2420-Å-Al–sapphire they find $\tau_0(\text{expt}) = 8\times10^{-6}$ sec in a steady-state experiment and $\tau_0(\text{expt}) = 2.8\times10^{-6}$ sec in a transient experiment.[60] Now the phonon-trapping effect, which makes the measured apparent recombination time longer than the intrinsic recombination time, increases with increasing acoustic mismatch between the film and the media on each side and increases roughly linearly with film thickness.[1] This is apparent in the difference between the experimental results for different substrates and film thicknesses. While it is impossible to determine with precision what intrinsic τ_0 these experimental data imply, an extrapolation to zero film thickness using estimates of the relative phonon transmissivities of Al-glass and Al-sapphire interfaces yields a τ_0 of about 1 μsec for the transient measurements and about 3 μsec for the steady-state measurements. The phonon trapping factors appear to be near one for vacuum–900-Å-Al–glass and near two for vacuum–2420-Å-Al–sapphire. These experimental τ_0's are, respectively, about 2 and 6 times our theoretical value of 438 nsec.

Smith and Mochel[61] have recently reported measurements of quasiparticle recombination times in Al using a tunnel-junction structure with and without a helium film covering one side of the structure. The phonon transmissivity of a superconductor/helium interface is known to be quite large[62] (0.25–0.5). Comparison of the two cases therefore permits in principle the independent determination of the phonon-trapping enhancement factor and the intrinsic recombination time. Smith and Mochel found an enhancement factor of 8.6 ± 1.1 for vacuum–900-Å-Al–glass and an intrinsic recombination time essentially identical to our theoretical value.[63]

The earlier results of Levine and Hsieh[64] appear to yield a value of τ_0 a factor of 2–6 smaller than our theoretical value, depending on what is assumed about the phonon-trapping factor in their experiments.

Chi and Langenberg[65] have recently measured the quasiparticle recombination time in Al using the microwave reflectivity technique of Sai-Halasz *et al.*[66] These experiments were done with very thin (300–400 Å) films on BaF_2 substrates. Under these conditions the phonon-trapping factor is expected to be very near one,[67] so that the observed recombination time should be close to the intrinsic recombination time. Measurements were made over the rather restricted temperature range $T/T_c = 0.80$–0.98. Over this range the observed times scatter around our present theoretical estimate within about a factor 2, and are thus

in agreement with theory to within that accuracy.

We conclude then that our theoretical estimate of the quasiparticle recombination time in Al is in agreement with existing experimental values to within about a factor 2, except perhaps for the results of Gray *et al.*[7,59] and Levine and Hsieh.[63]

Schuller and Gray[68] have studied quasiparticle recombination in Al at temperatures within several tens of millikelvins of T_c. In this temperature region fluctuations of the pair field appear to dominate the dynamics.[69] These pair field fluctuations are not taken into account in the calculations we have carried out. The nature of the apparently divergent lifetime observed by Schuller and Gray and its possible connection with the results of other experiments, including that of Peters and Meissner[70] on Sn, would appear to require further elucidation.

We have assembled the available experimental data for Sn in Fig. 18. The phonon-trapping effect for Sn is more severe than for Al because of its smaller phonon velocities and shorter recombination times. Most of the data thus represent effective or apparent recombination times which are substantially larger than the intrinsic recombination time. Note, however, the curve representing the upper limit on the intrinsic time obtained by Sai-Halasz *et al.*[66] by extrapolating data for films of various thickness to zero thickness in an attempt to eliminate the phonon-trapping effect. This lies quite close to our theoretical curve, indicating a reasonably satisfactory agreement between our theory and the available experimental information.

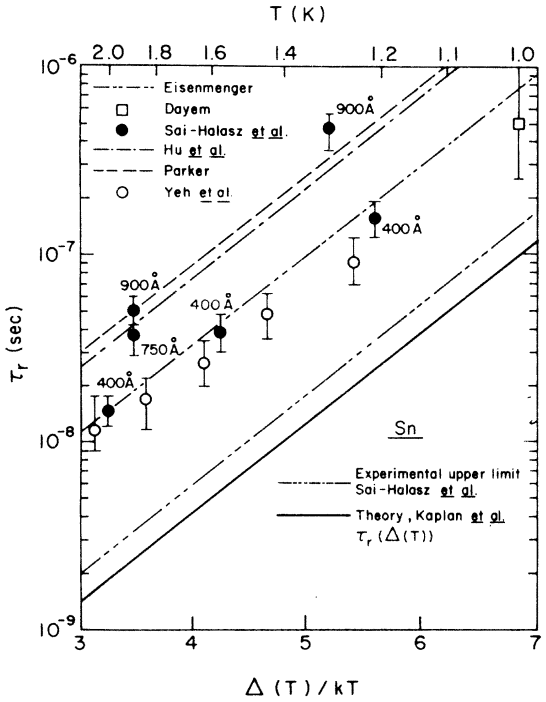

FIG. 18. Comparison of experimentally determined effective quasiparticle recombination lifetimes for Sn with theory. Experimental conditions, in the notation defined in the text, are: Eisenmenger (Ref. 71): helium–4000-Å–sapphire; Dayem (Ref. 72): helium–3000-Å–sapphire; Sai-Halasz *et al.* (Ref. 66): vacuum–indicated-thickness–quartz; Hu *et al.* (Ref. 73): helium–3200-Å–glass; Parker (Ref. 74): helium–3500-Å–sapphire. Yeh and Langenberg (Ref. 75): He–1600-Å–glass.

Jaworski *et al.*[76] have measured the effective (phonon-trapped) quasiparticle recombination time for Pb using the method of Ref. 74. For He–3500-Å-Pb–glass they report

$$\tau_{\text{eff}} = 2.06 \times 10^{-10} T^{-1/2} e^{\Delta(0)/kT} \text{ sec} ,$$

which is approximately 100 times larger than our theoretical value. No attempt was made to determine the phonon-trapping factor experimentally, but an estimate of this factor[76] yields a value very near 100, indicating that Jaworski *et al.*'s experimental recombination time and our theoretical recombination time are in quite satisfactory agreement.

E. Branch-mixing time

Clarke and Paterson[12,15] have made measurements of the relaxation of quasiparticle branch imbalance in Sn and Pb, using a technique in which the difference in the chemical potentials of pairs and a nonequilibrium tunnel-injected quasiparticle population is measured. Their experiments were analyzed using the theory of Tinkham and Clarke,[13,14] which incorporates the assumption $\tau_s \ll \tau_Q \ll \tau_r$. The remarks in Sec. IV about the relationship of τ_s, τ_Q, and τ_r indicate that this assumption is *never* strongly satisfied! This must be borne in mind in considering the experimental results. We must also remember that the times reported by Clarke and Paterson must be multiplied by two (cf. Sec. IV) before comparing with our theoretical times.

Experiments on the resistance of superconducting-normal interfaces near T_c,[30,31,77-79] and on phase-slip centers in superconducting microbridges, also near T_c,[80] yield a characteristic length which may be interpreted as a quasiparticle diffusion length $(\frac{1}{3} v_{qp} l \tau)^{1/2}$, where v_{qp} is an average quasiparticle velocity, l is the quasiparticle elastic scattering mean free path, and τ is some characteristic quasiparticle lifetime. While it is not yet completely clear which of our theoretical times is to be identified with τ, Yu and Mercereau[78] and Clarke[79] have identified τ with the branch-mixing time τ_Q. Assuming this is correct, we compare in Table III theoretical and experimental estimates

TABLE III. $\tau_Q(0)$ (sec). The times in columns one, three, and four are twice those reported in the references for the reason discussed in the text.

	Theory		Experiment	
	Tinkham	Kaplan *et al.* [c]	Tunneling	Superconducting-normal resistance
Sn	4×10^{-10} [a]	5.8×10^{-10}	2×10^{-10} [d]	6×10^{-10} [f]
Pb	8×10^{-12} [a]	4.3×10^{-11}	6×10^{-12} [e]	4×10^{-11} [f]
Ta	2.8×10^{-10} [b]	4.5×10^{-10}		1.3×10^{-10} [b]

[a] Reference 14.
[b] Reference 78.
[c] Present theory.
[d] Reference 15.
[e] Reference 15.
[f] Reference 79.

of $\tau_Q(0)$, defined by $\tau_Q=\tau_Q(0)\Delta(0)/\Delta(T)$ for T near T_c. There is considerable scatter, undoubtedly due to uncertainties in both experiment and theory, but the correspondence between our theory and experiment, especially the superconducting-normal interface resistance experiments, is quite good.

Tinkham's[14] theoretical estimate of τ_Q at low temperatures suggests that τ_Q decreases monotonically as T decreases, becoming essentially temperature independent for $T/T_c \lesssim 0.5$. This is in fact the behavior observed by Clarke and Paterson[15] for pure Sn. As noted in Sec. IV, however, Tinkham's estimate really applies only to fairly high energy quasiparticles. At energies near the gap edge, our results indicate that τ_Q passes through a minimum and then increases as T decreases (Fig. 11). Clarke and Paterson also studied Sn with 3 wt% In added to reduce gap anisotropy and hence the contribution of elastic scattering processes to the branch-mixing rate. This resulted in a general increase in τ_Q for $T/T_c \lesssim 0.9$ by about a factor 2. Moreover, inspection of their results for this "dirty" sample (Fig. 8 of Ref. 15) reveals a slight upturn in τ_Q with decreasing temperature. The data resemble the curve for $\omega = 2.5\Delta(0)$ in our Fig. 11. This suggests that quasiparticles were branch mixing predominantly from energies around $2-3\Delta(0)$ rather than nearer the gap edge. Since in this temperature region $2\tau_s \cong \tau_Q \ll \tau_r$, thermalization of the injected quasiparticles will not occur in times much shorter than branch mixing. Thermalization will therefore be incomplete and the typical energy of the branch-mixing quasiparticles may well be somewhat above (but not too far above) the gap edge, as suggested by the data. The strong dependence of τ_Q on energy at low temperature may provide a useful experimental test of some details of the distribution of the injected quasiparticles.

In preliminary experiments on Pb, Clarke and Paterson[15] observed a τ_Q which appeared to increase by nearly a factor 6 as T/T_c decreased from 0.6 to 0.2. They commented that this increase was "inconsistent with the theoretical predictions for τ_Q." Our results suggest that this is not necessarily the case; their experimental curve is a dead ringer for our theoretical curve (Fig. 13) at an energy slightly above $2\Delta(0)$. At 4.2 K ($T/T_c = 0.58$) their experimental τ_Q is about 6×10^{-12} sec; our theoretical value for $\omega = 2\Delta(0)$ is 2×10^{-11} sec. Considering the uncertainties of both experiment and theory, the quantitative agreement must be considered fairly good. Comparison of Figs. 11 and 12 shows that the experimentally observed large size of the low-temperature upturn in τ_Q for Pb as compared with Sn appears also in our theory; For $\omega = 2\Delta(0)$, the ratio of $\tau_Q(T=0)$ to τ_Q (min) is about five times larger for Pb than for the universal weak-coupling superconductor, and similar factors obtain at other energies.

F. Quasiparticle scattering in the normal state

In the rich and complex field of fermiology there are several types of experiments which can provide information on inelastic quasiparticle scattering from phonons.[81] These include surface Landau-level resonance (SLLR), radio frequency size effect (RFSE), and Azbel'-Kaner cyclotron resonance (AKCR) (but not, it should be noted, the de Haas–van Alphen effect). For each of these phenomena there are circumstances in which a single inelastic scattering event removes a quasiparticle from participation and thus contributes to the broadening of a resonance or impedance peak. The scattering rate can be inferred from the linewidth. In such circumstances, the relaxation rate is expected and observed to vary with temperature as $A+\gamma T^3$, where A represents temperature-independent scattering due to impurities, etc., and the T^3 term is the phonon scattering contribution. Hence γT_c^3 is precisely $\tau_s^{-1}(0,T_c)=\tau_r^{-1}(0,T_c)$, and comparison with Eq. (18) yields

$$\tau_0=\tfrac{7}{4}\Gamma(3)\zeta(3)/\gamma T_c^3=4.20/\gamma T_c^3. \tag{38}$$

This relation may be used to compare our τ_0's with γ's deduced from normal-metal experiments, with the following caution: The experiments named above measure quasiparticle scattering rates at specific points on the Fermi surface or averaged over specific cyclotron orbits on the Fermi surface. Hence, γ is in general highly anisotropic. In using Eq. (38) to generate a τ_0 for comparison with our averaged τ_0 one should restrict one's attention to those parts of the Fermi surfaces of the polyvalent superconductors which are most free-electron-like. Even then, the result should be viewed with some caution.

In Table IV, we compare some τ_0's derived from recent normal-metal experiments using Eq. (38) with our τ_0's from Table I. The agreement for Al and Zn is good and for In rather poor.

TABLE IV. $10^9\tau_0$ (sec).

Metal	Theory	Experiment	Source
In	0.799	3.3	RFSE, Ref. 82
		8.9	RFSE, Ref. 83
Al	438	620	SLLR, Ref. 84
Zn	780	720	AKCR, Ref. 85

ACKNOWLEDGMENTS

We would like to thank J. Clarke, W. H. Parker, and S. Gygax for the impetus their interest gave this work, J. Rowell for discussions of the low-energy $\alpha^2(\Omega)F(\Omega)$ tunneling data, and J. P. Carbotte for discussions of the theoretical calculations of $\alpha^2(\Omega)F(\Omega)$. We also thank R. C. Dynes, P. G. Tomlinson, and J. Clarke for providing data and preprints prior to publication, and K. E. Gray for pointing out to us the importance of the electron-electron interaction in such metals as Al. In addition, we are grateful to M. Cohen, T. C. Lubensky, and J. R. Schrieffer for stimulating discussions.

*Work supported by the Office of Naval Research and the National Science Foundation.

[1]For a recent review, see D. N. Langenberg, in *Low Temperature Physics-LT14*, edited by M. Krusius and M. Vuorio (American Elsevier, New York, 1975), Vol. V, p. 223.

[2]L. Tewordt, Phys. Rev. 127, 371 (1962); 128, 12 (1962).

[3]J. R. Schrieffer and D. M. Ginsberg, Phys. Rev. Lett. 8, 207 (1962).

[4]A. Rothwarf and M. Cohen, Phys. Rev. 130, 1401 (1963).

[5]K. E. Gray, Philos. Mag. 20, 267 (1969).

[6]V. G. Bar'yakhtar, V. F. Klepikov, and V. P. Seminozhenko, Fiz. Tverd. Tela 15, 1213 (1973) [Sov. Phys.-Solid State 15, 817 (1973)].

[7]K. E. Gray, J. Phys. F 1, 290 (1971).

[8]D. C. Lancashire, J. Phys. F 2, 107 (1972). Lancashire has pointed out the importance of electron-electron interactions for Al. We note, however, that a golden-rule calculation of electron-electron scattering, recombination and pair-breaking rates contains negative terms which he neglected. These terms, which are contained in a set of Feynman diagrams of the same order as the ones treated by Lancashire, represent quantum-interference (exchange) effects between scattered electrons. Moreover, the appropriate interaction is the sum of a large repulsive Coulomb term and a large attractive electron-phonon term, making it difficult to estimate the size of the relatively small net interaction.

[9]W. L. McMillan and J. M. Rowell, in *Superconductivity*, edited by R. D. Parks (Dekker, New York, 1969); J. M. Rowell, W. L. McMillan, and R. C. Dynes (unpublished).

[10]Because of the rapid variation in the tunneling density of states near the gap edge, tunneling data are generally not taken all the way to the gap. In the low-energy region where no data are available, the authors in Ref. 9 take $\alpha^2(\Omega)F(\Omega)$ proportional to Ω^2.

[11]D. J. Scalapino and B. N. Taylor [Bull. Am. Phys. Soc. 13, 475 (1968)] reported lifetime results for Pb obtained from $\alpha^2(\Omega)F(\Omega)$ in a manner similar to that discussed here. However, these results were never published.

[12]J. Clarke, Phys. Rev. Lett. 28, 1363 (1972).

[13]M. Tinkham and J. Clarke, Phys. Rev. Lett. 28, 1366 (1972).

[14]M. Tinkham, Phys. Rev. B 6, 1747 (1972).

[15]J. Clarke and J. L. Paterson, J. Low Temp. Phys. 15, 491 (1974).

[16]G. M. Eliashberg, Zh. Eksp. Teor. Fiz. 38, 966 (1960) [Sov. Phys.-JETP 11, 696 (1960)].

[17]D. J. Scalapino, in *Superconductivity*, edited by R. D. Parks (Dekker, New York, 1969).

[18]If $p = p_F$ so that $\epsilon_p = 0$ in Eq. (1), it follows that $-\mathrm{Im}\omega = -\mathrm{Im}\phi/Z \equiv -\Delta_2(\omega)$. Neglecting terms of second order in ϕ_2, Z_2 and their products, this is identical to $\Gamma(\Delta)$ given by Eq. (4).

[19]Our result, Eq. (6), differs from that of Tewordt (Ref. 2) in the manner in which the factors of Z enter, because our Z parameters are frequency dependent, while his are momentum dependent.

[20]P. B. Allen and M. L. Cohen, Phys. Rev. B 1, 1329 (1970).

[21]C. Kittel, *Introduction to Solid State Physics*, 4th ed. (Wiley, New York, 1971).

[22]Y. Nakagawa and A. D. B. Woods, Phys. Rev. Lett. 11, 271 (1963).

[23]G. Gladstone, M. A. Jensen, and J. R. Schrieffer, in *Superconductivity*, edited by R. D. Parks (Dekker, New York, 1969), Vol. II. Note that γ given in the fifth column of Table VI of this reference must be normalized by $Z_1(0)$ to yield $N(0)$, the electron den-

sity of states at the Fermi surface.
[24]J. P. Carbotte and P. G. Tomlinson, Phys. Rev. B 13, 4738 (1976).
[25]J. C. Swihart and P. G. Tomlinson (unpublished).
[26]C. S. Owen and D. J. Scalapino, Phys. Rev. Lett. 28, 1559 (1972).
[27]W. H. Parker, Phys. Rev. B 12, 3667 (1975).
[28]A. R. Long and C. J. Adkins, Philos. Mag. 27, 865 (1973).
[29]It is interesting to note that in the Pb calculations of Ref. 24, $Z_1(0)=2.32$ and $\alpha^2(2\Delta(0))F(2\Delta(0))$ is approximately half the experimental value of Ref. 9.
[30]A. B. Pippard, J. G. Shepherd, and D. A. Tindall, Proc. R. Soc. A 324, 17 (1971).
[31]G. L. Harding, A. B. Pippard, and J. R. Tomlinson, Proc. R. Soc. A 340, 1 (1974).
[32]The α for Sn which we estimate from Table I is about $\frac{2}{3}$ the estimate of Ref. 14.
[33]I. A. Privorotskii, Zh. Eksp. Teor. Fiz. 43, 1331 (1962) [Sov. Phys.-JETP 16, 945 (1963)].
[34]V. M. Bobetic, Phys. Rev. 136, A1535 (1964).
[35]J. A. Snow, Phys. Rev. 172, 455 (1968).
[36]G. T. Furukawa, T. B. Douglas, and N. Pearlman, in *AIP Handbook*, 3rd ed. (McGraw-Hill, New York, 1972).
[37]R. Stedman, L. Almqvist, and G. Nilsson, Phys. Rev. 162, 549 (1967).
[38]A. D. B. Woods, Phys. Rev. 136, 781 (1964).
[39]For a recent review of nuclear spin relaxation in superconductors, see D. E. MacLaughlin, in *Solid State Physics*, edited by H. Ehrenreich, F. Seitz, and D. Turnbull (Academic, New York, 1975), Vol. 31.
[40]M. Fibich, Phys. Rev. Lett. 14, 561 (1965); 14, 621 (1965).
[41]B. Mühlschlegel, Z. Phys. 155, 313 (1959).
[42]I. Giaever, H. R. Hart, Jr., and K. Megerle, Phys. Rev. 126, 941 (1962).
[43]S. Berman and D. M. Ginsberg, Phys. Rev. 135, A306 (1964).
[44]L. C. Hebel and C. P. Slichter, Phys. Rev. 113, 1504 (1957).
[45]Y. Masuda and A. G. Redfield, Phys. Rev. 125, 159 (1962).
[46]J. D. Williamson, Ph.D. thesis (University of California, Riverside, 1972) (unpublished).
[47]D. J. Scalapino and T. M. Wu, Phys. Rev. Lett. 17, 315 (1966); T. M. Wu, Ph.D. thesis (University of Pennsylvania, 1966) (unpublished).
[48]B. D. Josephson, Phys. Lett. 1, 251 (1962); Adv. Phys. 14, 419 (1965).
[49]E. Riedel, Z. Naturforsch. A 19, 1634 (1964).
[50]C. A. Hamilton and S. Shapiro, Phys. Rev. Lett. 26, 426 (1971).
[51]C. A. Hamilton, Phys. Rev. B 5, 912 (1972).
[52]S. A. Buckner, T. F. Finnegan, and D. N. Langenberg, Phys. Rev. Lett. 28, 150 (1972).
[53]S. A. Buckner and D. N. Langenberg, in *Low Temperature Physics-LT13*, edited by K. D. Timmerhaus, W. J. O'Sullivan, and E. F. Hammel (Plenum, New York, 1974), Vol. III, p. 285.
[54]S. A. Buckner and D. N. Langenberg, J. Low Temp. Phys. 22, 569 (1976).
[55]G. Vernet and R. Adde, Appl. Phys. Lett. 28, 559 (1976).
[56]H. Thomé and Y. Couder, in *Low Temperature Physics-LT14*, edited by M. Krusius and M. Vuorio (North-Holland, Amsterdam, 1975), Vol. IV, p. 156.
[57]B. Kofoed and K. Saermark, Phys. Lett. A 55, 72 (1975).
[58]A. Rothwarf and B. N. Taylor, Phys. Rev. Lett. 19, 27 (1967).
[59]K. E. Gray, A. R. Long, and C. J. Adkins, Philos. Mag. 20, 273 (1969).
[60]The steady-state experimental values quoted here have been increased by a factor $2Z_1(0)=2.86$ over those of Refs. 7 and 59 per K. E. Gray (private communication).
[61]L. N. Smith and J. M. Mochel, Phys. Rev. Lett. 35, 1597 (1975).
[62]See, for example, J. L. Gittleman and S. Bozowski, Phys. Rev. 128, 646 (1962).
[63]The experimental τ_0 of Ref. 61 has been increased by a factor of $2Z_1(0)=2.86$ per L. N. Smith (private communication).
[64]J. L. Levine and S. Y. Hsieh, Phys. Rev. Lett. 20, 994 (1968).
[65]C. C. Chi and D. N. Langenberg, Bull. Am. Phys. Soc. 21, 403 (1976); and unpublished.
[66]G. A. Sai-Halasz, C. C. Chi, A. Denenstein, and D. N. Langenberg, Phys. Rev. Lett. 33, 215 (1974).
[67]C. C. Chi, Ph.D. thesis (University of Pennsylvania, 1976) (unpublished).
[68]I. Schuller and K. E. Gray, Phys. Rev. Lett. 36, 429 (1976).
[69]A. Schmid and G. Schön, J. Low Temp. Phys. 20, 207 (1975).
[70]R. Peters and H. Meissner, Phys. Rev. Lett. 30, 965 (1973).
[71]W. Eisenmenger, in *Tunneling Phenomena in Solids*, edited by E. Burstein and S. Lundqvist (Plenum, New York, 1969), p. 371.
[72]A. H. Dayem, J. Phys. (Paris) Suppl. 33, 15 (1972).
[73]P. Hu, R. C. Dynes, and V. Narayanamurti, Phys. Rev. B 10, 2786 (1974).
[74]W. H. Parker, Solid State Commun. 15, 1003 (1974).
[75]J. T. C. Yeh and D. N. Langenberg, Bull. Am. Phys. Soc. 21, 404 (1976); and unpublished.
[76]F. Jaworski, W. H. Parker, and S. B. Kaplan, Phys. Rev. B 14, 4209 (1976).
[77]M. L. Yu and J. E. Mercereau, Phys. Rev. Lett. 28, 1117 (1972).
[78]M. L. Yu and J. E. Mercereau, Phys. Rev. B 12, 4909 (1975).
[79]J. Clarke (private communication).
[80]W. J. Skocpol, M. R. Beasley, and M. Tinkham, J. Low Temp. Phys. 16, 145 (1974).
[81]See J. F. Koch and R. E. Doezema, in *Low Temperature Physics-LT14*, edited by M. Krusius and M. Vuorio (North-Holland, Amsterdam, 1975), Vol. V, p. 314, and references therein.
[82]I. P. Krylov and V. F. Gantmakher, Zh. Eksp. Teor. Fiz. 51, 740 (1966) [Sov. Phys.-JETP 24, 492 (1966)].
[83]P. M. Snyder, J. Phys. F 1, 363 (1971).
[84]R. E. Doezema and T. Wegehaupt, Solid State Commun. 17, 631 (1975).
[85]D. M. Brookbanks, J. Phys. F 3, 988 (1973).